THE EFFECTS OF ACCELERATION ON BURNING RATES OF NONMETALLIZED COMPOSITE PROPELLANTS

by

Robert Carroll Bates

United States
Naval Postgraduate School

THESIS

THE EFFECTS OF ACCELERATION ON BURNING RATES
OF NONMETALLIZED COMPOSITE PROPELLANTS

by

Robert Carroll Bates

October 1969

The Effects of Acceleration on Burning Rates of Nonmetallized Composite Propellants

by

Robert Carroll Bates
Lieutenant, United States Navy
B.S., United States Naval Academy, 1962

Submitted in partial fulfillment of the
requirements for the degree of

MASTER OF SCIENCE IN AERONAUTICAL ENGINEERING

from the
NAVAL POSTGRADUATE SCHOOL
October 1969

ABSTRACT

The burning rates of five nonmetallized composite propellants were measured in acceleration fields up to 1000g using a combustion bomb mounted on a centrifuge. Two propellants were burned at 1000 psia and all five were burned at 500 psia.

The experimental results were examined to separate the effects of pressure, base burning rate and AP crystal size on burning rate augmentation. Increasing pressure was found to increase the augmentation except at low acceleration levels. The augmentation was found to be a strong function of base burning rate and a weak function of AP crystal size.

The results were compared with Sturm's model for augmentation of nonmetallized composite propellants and found to compare favorably. A new expression for $d_{critical}$ was proposed which better correlates experimental data.

TABLE OF CONTENTS

I. INTRODUCTION ---------- 11

II. EXPERIMENTAL EQUIPMENT AND PROCEDURES ---------- 13

A. EXPERIMENTAL EQUIPMENT ---------- 13

B. EXPERIMENTAL PROCEDURES ---------- 21

III. PROPELLANTS, STRAND PREPARATION AND DATA REDUCTION ---------- 27

A. PROPELLANTS ---------- 27

B. STRAND PREPARATION ---------- 29

C. DATA REDUCTION ---------- 31

IV. REVIEW OF STURM'S MODEL ---------- 34

V. EXPERIMENTAL RESULTS AND DISCUSSION ---------- 41

A. GENERAL DISCUSSION ---------- 41

B. EFFECT OF PRESSURE ON AUGMENTATION ---------- 50

C. EFFECT OF AP SIZE AND BASE BURNING RATES OF AUGMENTATION ---------- 54

D. EFFECT OF BASE BURNING RATE ON AUGMENTATION ---------- 57

E. EFFECT OF AP SIZE ON AUGMENTATION ---------- 60

F. COMPARISON OF DATA WITH STURM'S MODEL ---------- 63

VI. CONCLUSIONS ---------- 69

REFERENCES ---------- 70

INITIAL DISTRIBUTION LIST ---------- 71

FORM DD 1473 ---------- 73

LIST OF TABLES

TABLE		PAGE
I.	Propellant Formulations	27
II.	Data for Propellant N-1	43
III.	Data for Propellant N-2	45
IV.	Data for Propellant N-3	46
V.	Data for Propellant N-4	48
VI.	Data for Propellant N-5	49

LIST OF FIGURES

FIGURE		PAGE
1.	Overhead Oblique View of Centrifuge	14
2.	Nitrogen Charging Station	15
3.	Engine Control Console	17
4.	Standard Strand Holder	18
5.	Pressure Sensing and Recording Circuit	20
6.	Timing Wire, Ignition and Continuity Test Circuits	22
7.	Instrumentation Console	23
8.	Placing Strand Holder in Combustion Bomb	25
9.	Ammonium Perchlorate Size Distribution	28
10.	Typical Pressure-Time Trace	32
11.	Phalanx Flame at Steady State	35
12.	Effect of Pressure on Burning Rate Augmentation of Non-Metallized Composite Propellant (N-1)	51
13.	Effect of Pressure on Burning Rate Augmentation of Non-Metallized Composite Propellant (N-3)	52
14.	Effect of AP Size and Base Burning Rate on Burning Rate of Non-Metallized Composite Propellants at 500 psia	55
15.	Effect of AP Size and Base Burning Rate on Burning Rate Augmentation of Non-Metallized Composite Propellants at 500 psia	56
16.	Effect of Base Burning Rate on Burning Rate of Non-Metallized Composite Propellants at 500 psia	58
17.	Effect of Base Burning Rate on Burning Rate Augmentation of Non-Metallized Composite Propellants at 500 psia	59
18.	Effect of AP Size on Burning Rate of Non-Metallized Composite Propellants at 500 psia	61

FIGURE PAGE

19. Effect of AP Size on Burning Rate Augmentation of Non-Metallized Composite Propellants at 500 psia ----- 62

20. Comparison of Stokes' vs. Non-Stokes' Theory with Experiment for P410 Propellant ---------- 67

21. Comparison of Stokes' vs. Non-Stokes' Theory with Experiment for P411 Propellant ---------- 68

ACKNOWLEDGMENTS

The author wishes to express his appreciation to Mr. Gene Woodford for the graphics work and to Mr. Edward Michelson for his assistance during the experimental portion of this investigation.

The author is especially indebted to his advisor, Dr. David Netzer, whose patience and guidance during the course of this investigation were greatly appreciated.

This investigation was sponsored by the Naval Ordnance Systems Command, Navweps 4235/6.

I. INTRODUCTION

The performance characteristics of solid propellant rocket motors have proven to be affected by the acceleration loads imposed on the burning propellant during spin-stabilized flight. As reported by several investigators [1, 2, 3], non-metallized composite solid propellants are affected significantly by the forces of acceleration which are directed normal to and into the burning surface. Acceleration induced changes in burning rate result in a definite deterioration in the rocket's performance, and produce changes in motor operating pressure, propellant burn time, and propellant burning characteristics. Therefore, to capably design a rocket motor which is subjected to the effects of acceleration, the effects must be known and understood.

Nonmetallized composite propellants with unimodal ammonium perchlorate (AP) were investigated to determine the effects of acceleration on the burning rates. The following effects were investigated: 1) pressure; 2) AP crystal size; and 3) base burning rate (burning rate at 0g). These effects were investigated because Sturm's [2] model predicts that they affect the burning rate of a nonmetallized composite propellant when it is subjected to an acceleration force. A unimodal AP crystal size was used in order to isolate the effects of this parameter. The parameters of AP crystal size and base burning rate were varied using five different propellants in order to study the combined and separate effects of each. The base burning rate was varied by the use of a catalyst.

The data reported by various investigators [2, 4, 5] indicate that both metallized and nonmetallized composite propellants exhibit

acceleration sensitivity. It is therefore doubtful that the acceleration sensitivity of aluminized composite propellants can be entirely attributed to the presence of the aluminum. By isolating the effect of the AP crystal size in nonmetallized composite propellants, the extent to which the AP crystal size effects the total propellant acceleration sensitivity of aluminized composite propellants can be determined.

The idea of opposing acceleration and drag forces on the solid oxidizer particles as proposed by Sturm [2] needs further investigation. After the effects of pressure, AP crystal size, and base burning rate were determined experimentally, they were compared with Sturm's model both from a physical and analytical standpoint.

In Section II, a brief discussion is presented of the centrifuge and related equipment, and of the experimental techniques utilized in this study. The propellant formulations, the preparation of the propellant strands, and the method of data reduction are presented in Section III. In Section IV, a brief review of Sturm's physical and analytical model is presented. The experimental results and discussion along with a comparison of the results with Sturm's model are presented in Section V. In Section VI, certain conclusions are drawn from the results of this investigation.

II. EXPERIMENTAL EQUIPMENT AND PROCEDURES

A. EXPERIMENTAL EQUIPMENT

1. General

The investigation was conducted at the Naval Postgraduate School Rocket Test Facility. The centrifuge test facility consists of a centrifuge, engine control,and instrumentation consoles, and a nitrogen charging station. The centrifuge and nitrogen charging station were located in one test cell while the two consoles were located in the control and instrumentation room of the facility. A centrifuge-mounted combustion bomb was employed to study the effects of acceleration and pressure on the burning rates of solid propellants. The design of the system affords essentially constant pressure and acceleration levels during experimental runs. A complete description of the facility is contained in Reference 6 with modifications made to it in References 2 and 7. Therefore, only a general description of the system will be presented.

2. Centrifuge

Figure 1 shows an overhead oblique view of the centrifuge. The combustion bomb is mounted on the centrifuge arm at a radius of three feet and is connected to two surge tanks located near the centrifuge centerline. The centrifuge and bomb can be used to study the burning rates of propellant strands from atmospheric pressure to 1500 psia and from zero to 2,000 g's. The nitrogen charging station is shown in Figure 2. A total bomb and surge tank volume of 1,565 cubic inches allowed experiments to be conducted with practically a constant pressure. The largest pressure variation encountered was

ENLARGE

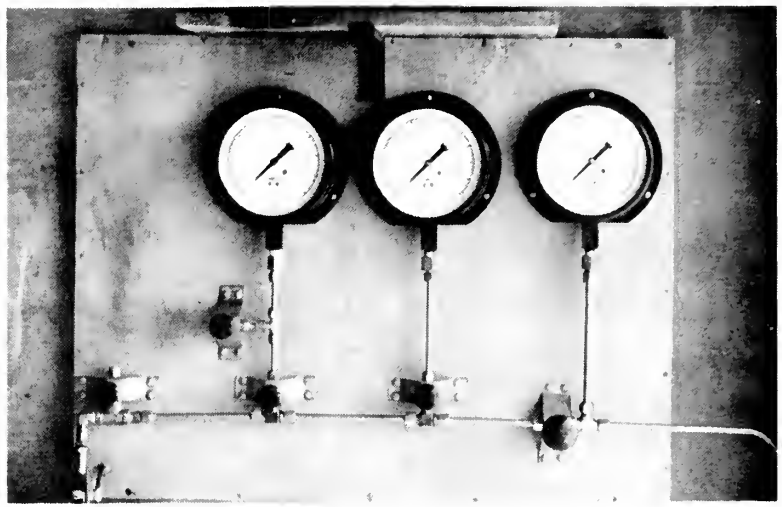

less than 6 per cent. For the 2-inch strand lengths used, the variation in the acceleration field during an experimental run was less than 6 per cent due to the relatively large radius of the centrifuge arm.

The centrifuge is powered by a conventional automobile engine. The speed of the centrifuge was controlled from the engine control console shown in Figure 3. The structural part of the rotor assembly is 3/4" aluminum plate, and it supports the stainless steel combustion bomb, the surge tanks, associated stainless steel tubing, valves, fittings, a pressure transducer, and counter-weights.

3. Strand Holders

The propellant strand holders consisted of a machined aluminum plug, canvas-phenolic strand support, and a commercial gland seal for the ignition wire. The aluminum plug was a slip-fit in an access port in the combustion bomb, and was locked in place with an aluminum collar. Figure 4 shows a schematic drawing of the strand holder.

4. Instrumentation

Instrumentation was provided to determine centrifuge rotational speed, pressure rise in the combustion bomb, and propellant burn time. The centrifuge rotational speed was needed to determine the acceleration force on the propellant. The pressure rise was used to determine the absolute pressure exerted on the propellant during a test. The propellant burn time was needed to determine the average propellant burning rate.

A SPACO type PA-I magnetic pickup was used to sense the centrifuge rotational speed. The SPACO output signal was transmitted to a Berkeley Model 5545 EPUT meter which was located on the engine control

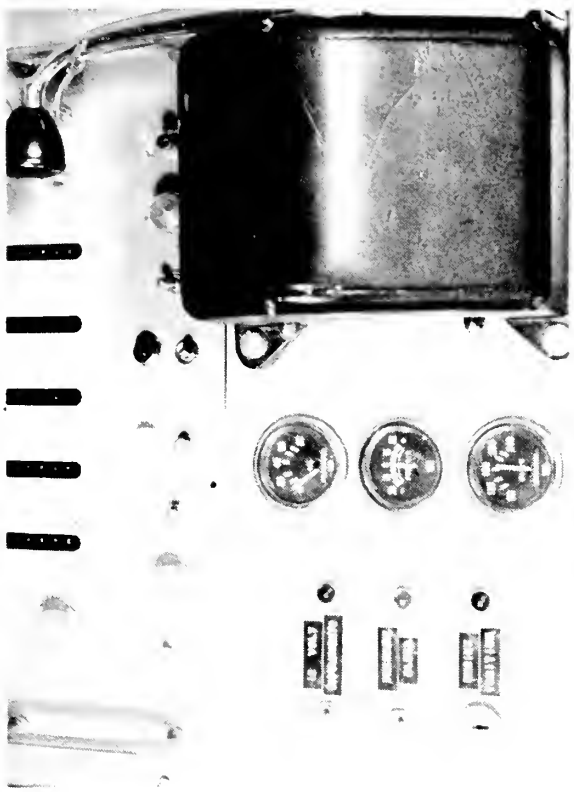

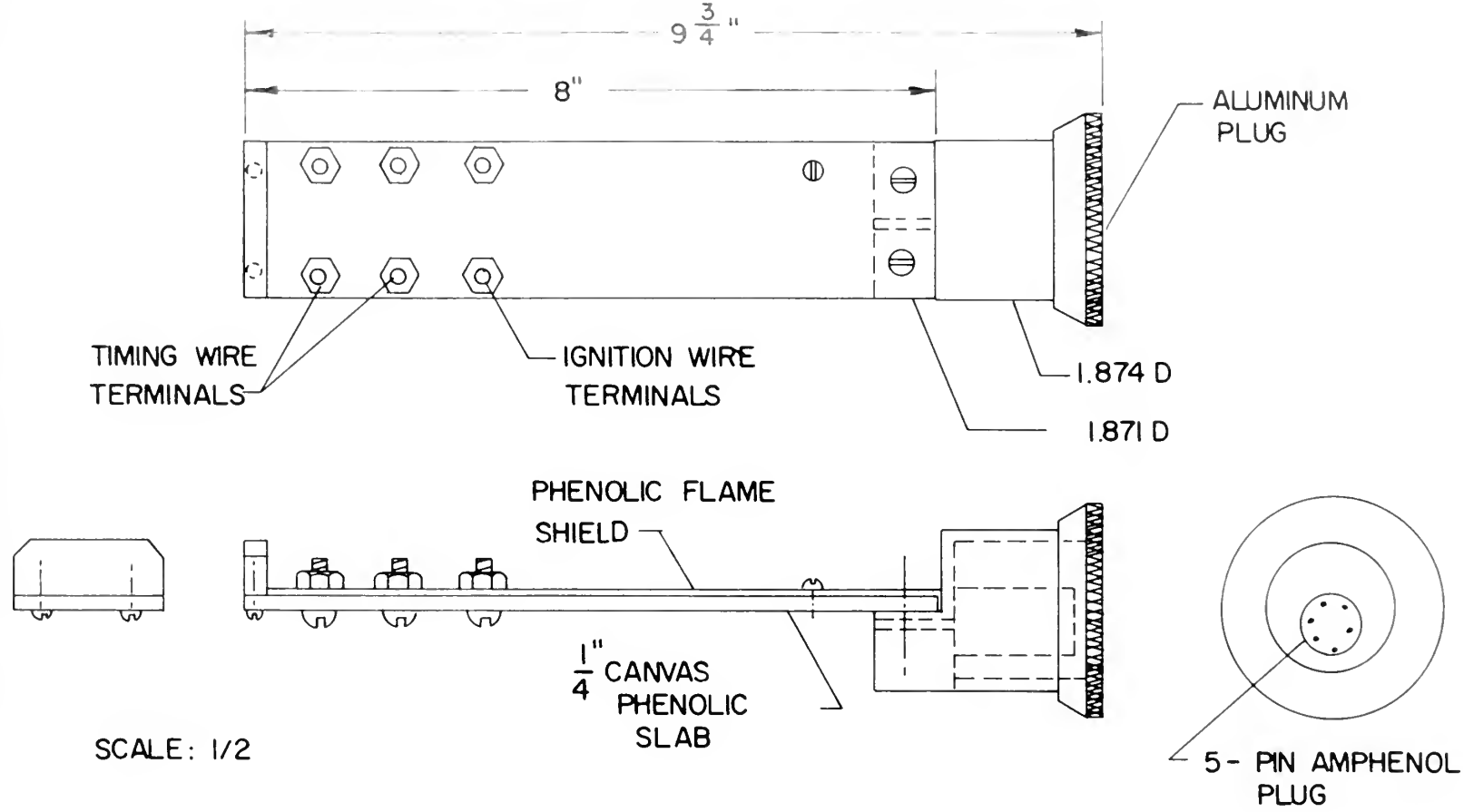

FIGURE 4

STANDARD STRAND HOLDER

console. The EPUT meter was checked before and after the series of tests and it was found to have a maximum error of 1 per cent.

Pressure rise in the bomb was sensed by a Daystrom-Wiancko type P2-1251 variable reluctance pressure transducer. The transducer was mounted on the rotor arm over the center of rotation to minimize acceleration effects. Transducer excitation voltage was supplied by a Model 3569, transistorized power supply, from Systems Research Corporation. The transducer output signal was amplified by an Astro Data Model 885 wide-band differential amplifier. The voltage signal from the amplifier was then displayed on a Honeywell Model 1508 Visicorder. A bucking voltage was used to cancel the signal from the transducer due to the initial pressure in the combustion bomb-surge tank system. Therefore, a zero reading was displayed on the Visicorder prior to propellant burning and only the pressure rise during propellant burn was recorded. The variable bucking voltage to the transducer output was supplied by a 22 volt dry-cell battery and a potentiometer. A 20,000 ohm variable resistor was used to allow adjustment of the Visicorder scale. Figure 5 shows the pressure sensing and recording circuit.

A 20 hertz time-base was recorded on the Visicorder chart during an experimental run. The time base was provided by a Hewlett-Packard Model 211A square wave generator. The 20 hertz output signal of the generator drove a M 200-120 galvanometer in the Visicorder. The output of the generator was calibrated before each run sequence with a Berkeley Model 5545 EPUT meter.

The propellant sample was ignited by means of a 12-volt d.c. power supply. A mixture of Testors Household Cement and black powder,

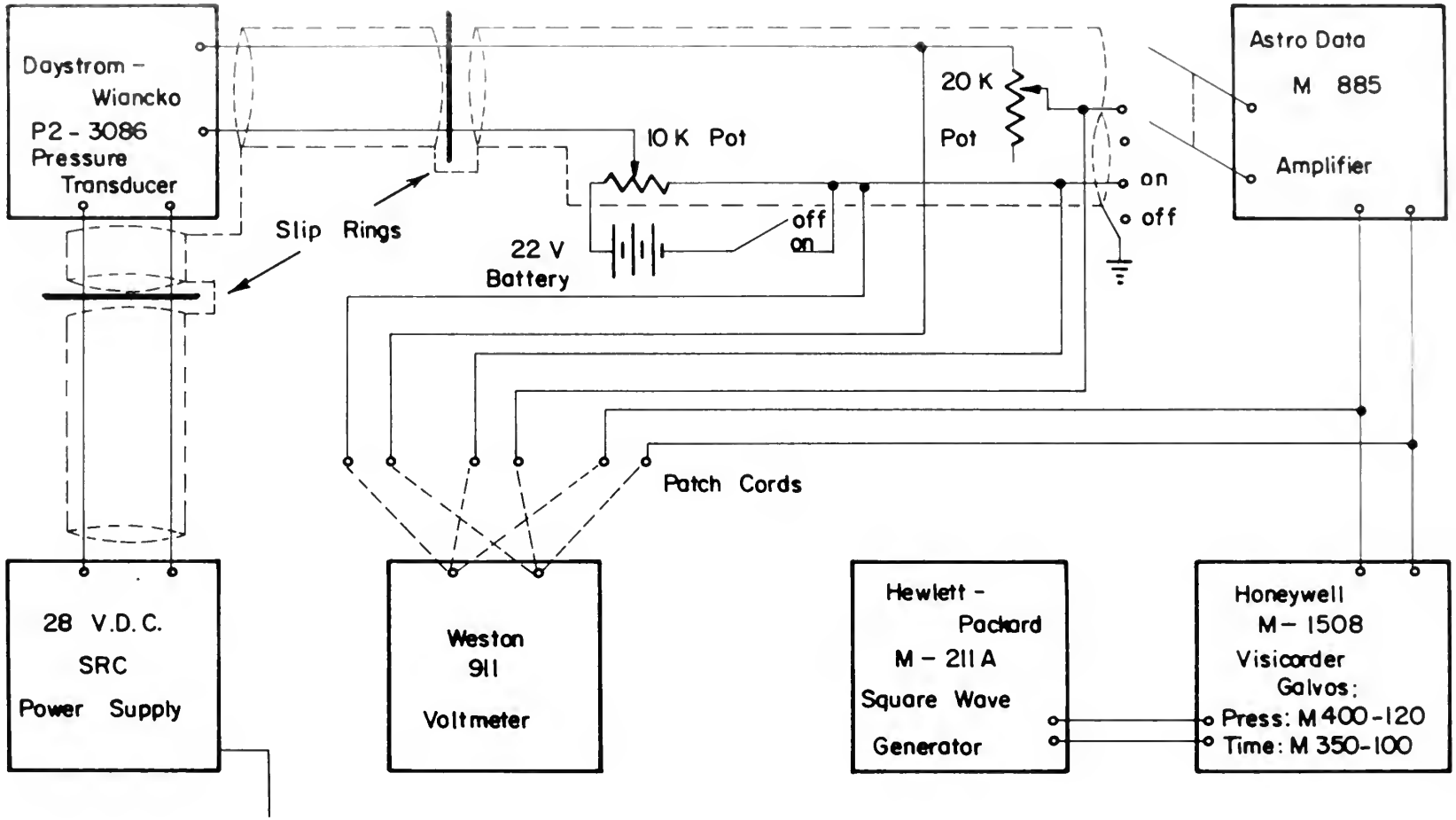

FIGURE 5

PRESSURE SENSING AND RECORDING CIRCUIT

which was affixed to the exposed end of the propellant, was ignited by the ohmic heating of a number 32 nichrome wire which was attached to the ignition wire terminals of the strand holder.

Figure 6 shows a schematic drawing of the ignition, timing, and continuity test circuits. The timing circuit was not utilized in this investigation. Figure 7 is a picture of the instrumentation console.

5. Nitrogen Charging System

The nitrogen charging system consisted of four bottles containing compressed nitrogen connected by a manifold, a pressure regulator, a gauge panel, a flexible charging hose, and stainless steel tubing. The gauge panel consisted of three Marsh Type 220-35 pressure gauges with ranges of 0-1000 psig, 0-3000 psig, and 0-5000 psig. The system was arranged to permit selection of that gauge from which one could most accurately monitor the pressurization of the surge tanks and combustion bomb.

B. EXPERIMENTAL PROCEDURES

A detailed description of experimental procedures is described in References 2 and 7, and therefore only a brief description is presented herein.

A one hour warm-up and stabilization period was allowed for all equipment and instrumentation except the transducer excitation power supply. It was determined that the voltage from it was breaking down the centrifuge brushes which transmitted the transducer signal to the amplifier and producing a noisy pressure-time trace. It was therefore left in the OFF condition until just prior to commencement of firings.

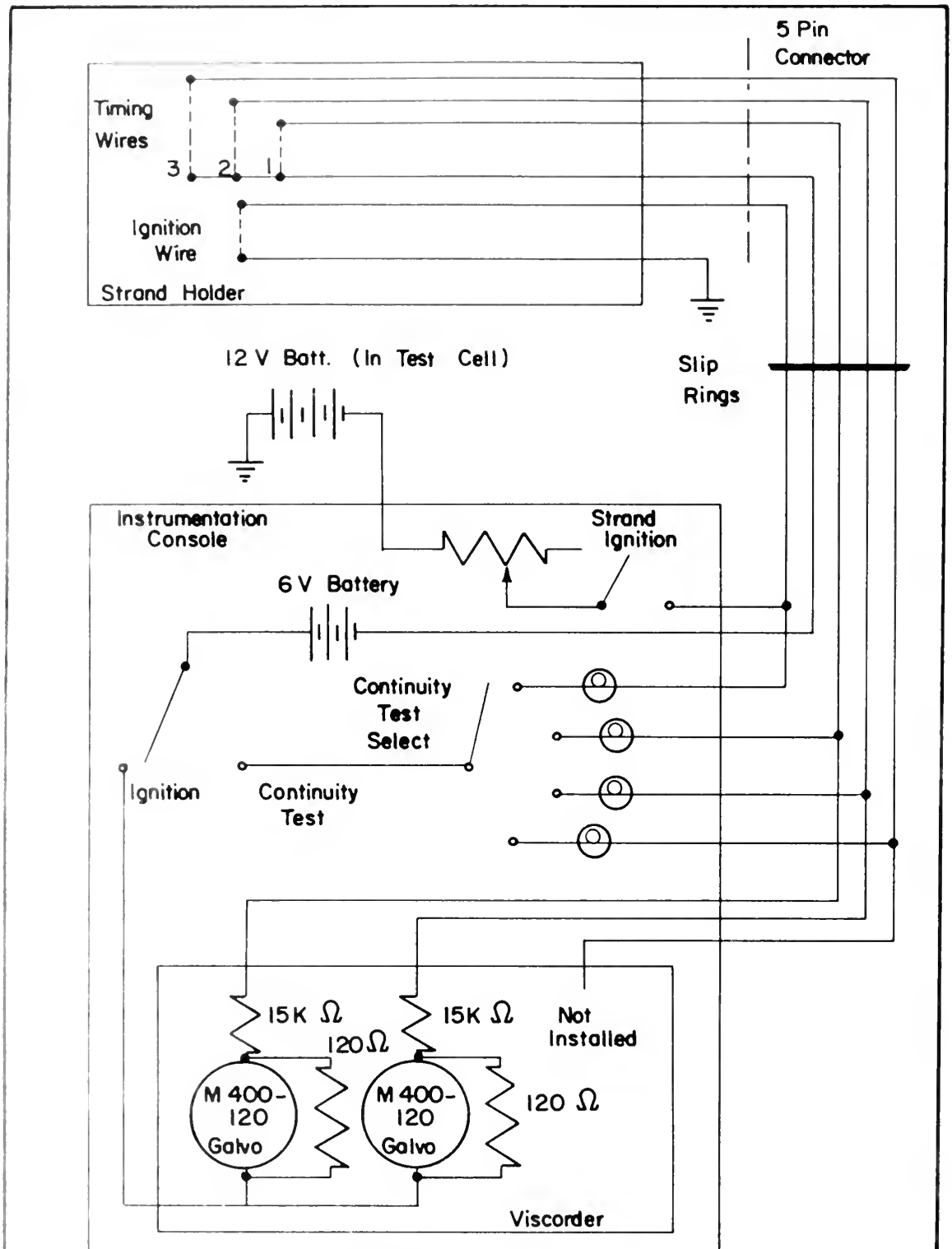

FIGURE 6

TIMING WIRE, IGNITION AND CONTINUITY TEST CIRCUITS

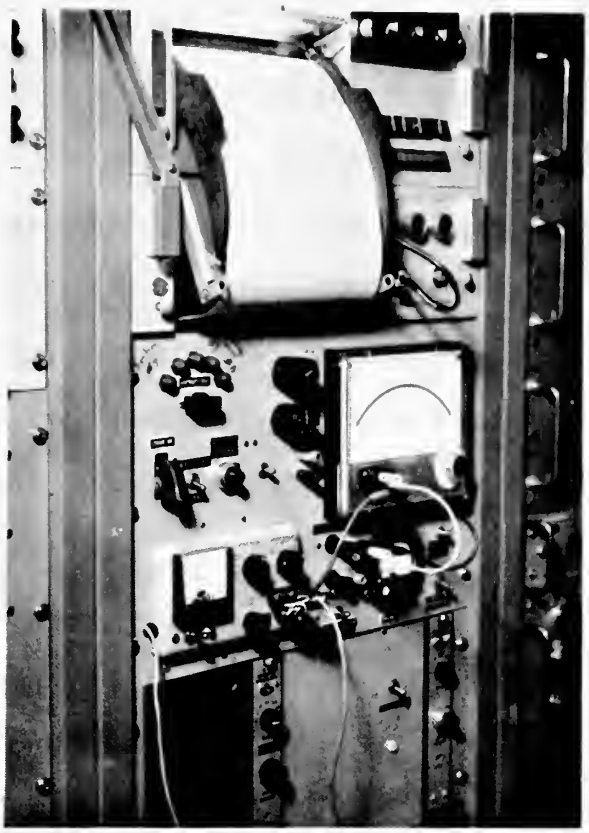

FIGURE 7. INSTRUMENTATION CONSOLE

The strands were removed from a glass desiccator jar and mounted on a strand holder. The strand holder was then placed in the combustion bomb as shown in Figure 8 and the combustion bomb was sealed. All experimental runs were made with the propellant at room temperature. Continuity of the strand ignition circuit was checked. The surge tank-combustion bomb system was then pressurized to the desired gauge pressure at the charging station. This gauge pressure was determined according to the absolute bomb pressure desired in the following manner:

$$p(\text{psig}) = p(\text{psia}) - 15 - \Delta p_g + 10 - \Delta P_m \qquad (1)$$

where

$p(\text{psig})$ = gauge pressure set at nitrogen charging station

$p(\text{psia})$ = average absolute pressure desired in the bomb for the experimental run

$15(\text{psia})$ = approximate atmospheric pressure

ΔP_g = correction for increased pressure in bomb due to centrifugal force (Reference 6)

$10(\text{psig})$ = approximate pressure differential required to unseat the charging valve on the rotor

ΔP_m = expected average pressure rise during test.

The rotor was engaged and while being brought to the desired speed, the chart speed and amplifier gain were set. A chart speed of from 2 to 4 inches per second was used on all experimental runs. Amplifier gain was adjusted to give about 4 to 5 inches of deflection on the Visicorder due to the pressure rise during propellant burn. The values of chart speed gave from 8 to 25 inches of chart travel.

The desired speed of the centrifuge was selected in terms of g-load desired. As stated in Reference 6 the relation between the two for a 2-inch strand length is:

$$N = 15.72\ G^{\frac{1}{2}} \qquad (2)$$

where

$N = \left(\frac{RPM}{2}\right)$ value displayed at the engine control console.

$G = \frac{\text{acceleration}}{g}$

g = acceleration due to gravity

When the centrifuge speed had stabilized, the Visicorder chart drive was turned on and allowed to run for about 2 seconds to stabilize. The propellant strand was then ignited by closing the ignition switch. After ignition of the black powder was observed, the ignition switch was opened. After propellant burn-out was observed, the Visicorder chart drive was turned off and the engine throttle was closed.

During the propellant burn time, the centrifuge speed was held to a variation of $\pm$ 2 rpm which allowed maximum errors of 1g at 50g and 8g at 1,000 g..

A data sheet was kept for each run and contained the data, propellant type, strand length, and cross-section measurements, initial propellant temperature, chart speed, amplifier gain, initial bomb pressure, and the N reading obtained during firing. The pressure-time trace chart was marked with a test identification number which was also marked on the data sheet.

III. PROPELLANTS, STRAND PREPARATION, AND DATA REDUCTION

A. PROPELLANTS

Five different propellants were used during this investigation. All five were nonmetallized composite propellants with unimodal AP. The propellant designations and formulations are summarized in Table 1.

TABLE I.

PROPELLANT FORMULATIONS

Propellant Designation	Weight % AP	AP Size (μ)	Weight % PBAN	Weight % Fe_2O_3
N-1	79.00	9	21.00	-
N-2	79.00	90	21.00	-
N-3	79.00	420	21.00	-
N-4	78.21	90	20.79	1.00
N-5	77.42	90	20.58	2.00

All ammonium perchlorate was supplied by the American Potash and Chemical Corporation. The 9μ AP was used as supplied and had a measured particle size of 8.2 to 9.4 μ. The 90μ AP was also used as supplied. A diameter distribution is shown in Figure 9 for the 90μ AP. The large AP passed a Tyler #32 mesh (500μ) and what held on a Tyler #35 mesh (420μ) was used. The iron oxide employed had the following specifications:

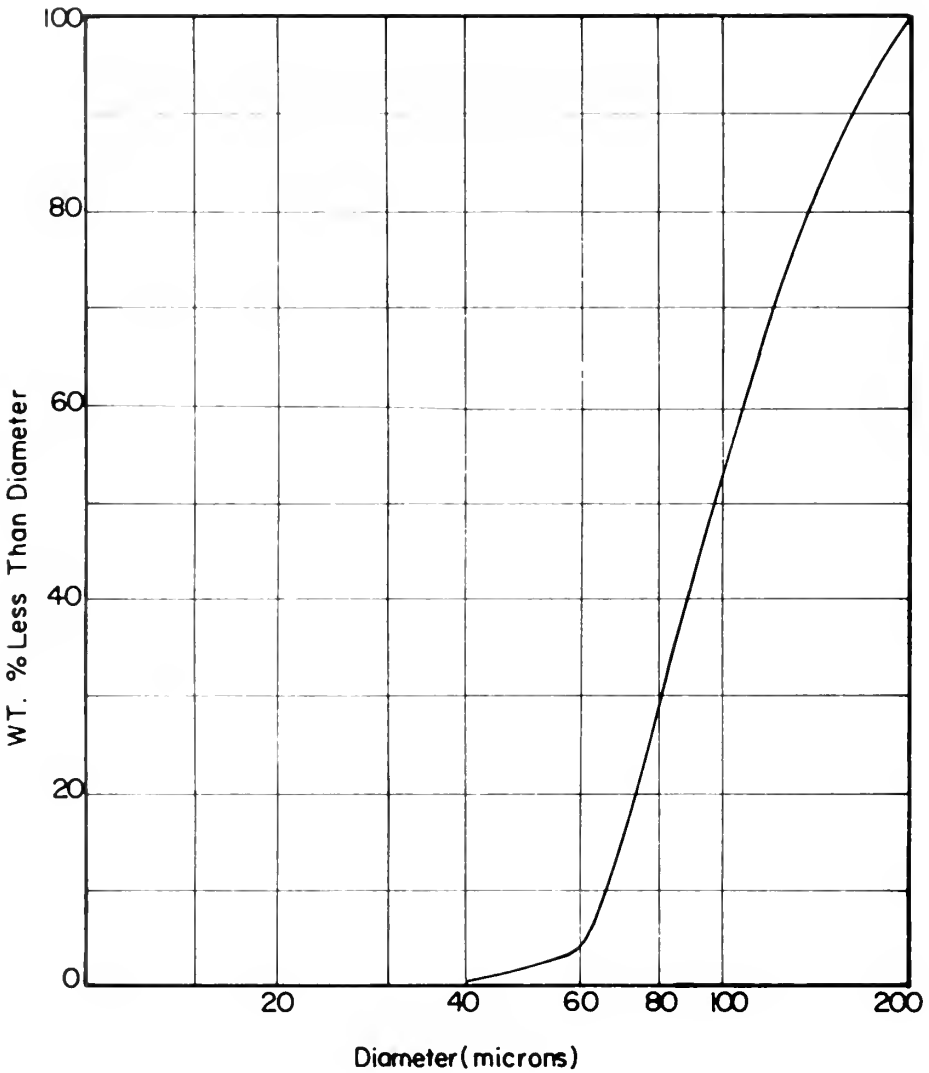

FIGURE 9. AMMONIUM PERCHLORATE SIZE DISTRIBUTION.

Physical description - Yellow light lemon elongated particles

Chemical composition - Hydrated Fe_2O_3

Average particle diameter - 0.40 microns

Density - 3.401 gm/cc

A weight ratio of 79 parts AP to 21 parts PBAN was maintained in all five propellants.

B. PROPELLANT STRAND PREPARATION

The five propellants were received in cardboard containers measuring about 5 x 3 x 8 inches. The solid block of propellant was cut into 1/2 x 1/2 inch cross section strands which were about 5 inches long. The strands were cut using a jig to obtain an even and accurate cut. A 90-inch Delta bandsaw was used for the cutting of the strands. An attempt was made to x-ray the strands using a Norelco Search Ray X-ray machine to check for voids which might have formed during the manufacture of the propellants. This was unsuccessful. It was decided to run the experiments repeatedly until the data obtained were consistent.

The strands were then placed in a mold which allowed it to be enclosed in an inhibitor on all four sides. The mold provided a 1/8 inch thick inhibitor. The inhibitor used on the strands was an unsaturated polyester resin cured with a peroxide. The resin used was Selection 5119 (Pittsburg Plate Glass Company). The curing agent was a 60 per cent solution of methyl ethyl Keytone and cyclohexanone peroxides in dimethyl phthalate ("Norox," Noroc Company, Azusa, California). A weight ratio of 24 resin to 1 of curing agent was

used. The mixture was thoroughly stirred and then poured over the strands in the mold. The inhibitor cured at room temperature and required approximately three hours.

The strands were then taken out of the molds and cut on the bandsaw to approximately 2 inch lengths. The strands were cut so that there was no inhibitor on the ends of the strands. The strand length was then measured with a micrometer to within .001 of an inch. One end of the strand was wrapped with scotch tape over masking tape to serve as a mold and the end was capped with the same inhibitor mixture as mentioned previously. The strands were then stored in a glass desiccator jar until used for the experimental runs.

In order to prepare the strands for firing, the inhibitor free end of the strands were notched on each side of the inhibitor case about about 1/16 inch below the propellant surface. This was done to provide a groove in which to place the ignition wire. A piece of number 32 nichrome wire was attached to one of the ignition wire terminals, the strand placed on the holder and then the other end of the wire attached to the other ignition wire terminal. The wire was placed in the grooves on the inhibitor case so it was not touching the propellant. A spacer was inserted between the end of the strand holder and the capped end of the strand to locate the open end of the strand even with the ignition wire terminals. The strand was secured to the strand holder by masking tape and labeled with its identifying number. A mixture of black powder and Testors Household Cement was then affixed to the exposed end of the propellant. The strand holder was then checked for continuity.

C. DATA REDUCTION

1. Determination of the Acceleration Field

For a constant centrifuge rpm the acceleration field which exists on the propellant is composed to two components: a radial component dependent on the angular velocity and the radial distance to the propellants surface, and a vertical component due to the earth's gravitational field. The lowest level of acceleration employed during the investigation was 50 times the standard acceleration due to gravity. Therefore the vertical component was neglected and the only acceleration acting on the propellants surface was considered to act horizontally into the surface and equal to the radial component.

Since 2 inch strand lengths were used exclusively, Equation 2 gave the correct relationship between rpm and acceleration.

2. Determination of Propellant Burning Rates

Figure 10 shows a typical pressure-time trace obtained on the Visicorder chart. Propellant ignition was determined to occur 1/20 second after black powder ignition. It was experimentally determined that this was the time required for the black powder to completely burn across the face of the propellant. Propellant burn-out occurred when the pressure ceased to increase in the bomb. The time between ignition and burn-out was determined from the 20 cps reference signal displayed adjacent to the pressure-time trace. The length of the strand was divided by the total propellant burn time to obtain the average propellant burning rate.

A polar planimeter was used to obtain the area under the pressure-time trace in square inches. The mean pressure rise due to propellant burn was determined according to the following equation:

$$P_b = \frac{AC}{L} \qquad (3)$$

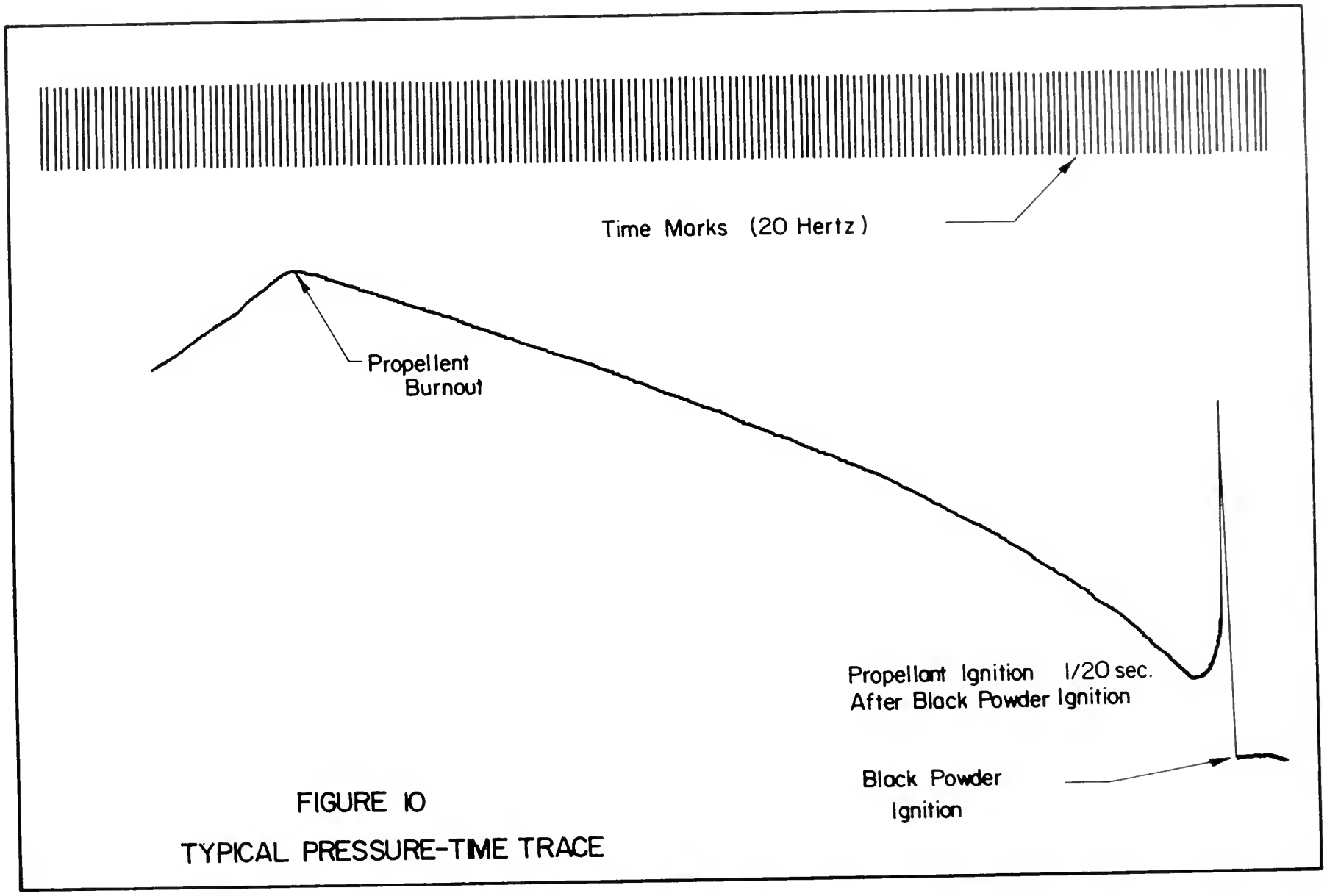

FIGURE 10

TYPICAL PRESSURE-TIME TRACE

where:

ΔP_b = Mean pressure rise during propellant burn (psi)

A = Area under pressure-time trace (in^2)

C = Calibration of transducer, dependent on amplifier gain (psi/in)

L = Length of pressure-time trace (in.)

Using Equation 1, the average absolute pressure that existed for the burning rate experiment can be found. Using Equation 2, the G level that existed for the experiment can be determined. The augmentation was defined as follows:

$\frac{\dot{r}}{\dot{r}_o}$ = Augmentation

where

$\dot{r}$ = burning rate at a given g level and pressure (in/sec)

$\dot{r}_o$ = burning rate at 0g and at the same given pressure (in/sec)

Allowing a possible 1 cycle error for both the determination of propellant ignition and the propellant burn-out, the probable uncertainty in the burning rate measurement was within 2 per cent.

IV. REVIEW OF STURM'S MODEL

A. PHYSICAL MODEL

Sturm [2] proposed a model to predict the effects of acceleration on the burning rates of nonmetallized composite propellants. Another model has been proposed by Glick [8] for nonmetallized composite propellants. He proposed an extension to Summerfield's granular diffusion flame model [9] to include acceleration effects. The model, however, fails to correctly predict the effects of acceleration on the burning rates of nonmetallized composite propellants.

Sturm extended Fenn's model [10] for the burning of composite propellants to include acceleration effects. Fenn represented the flame as burning in a gaseous reaction zone centered between streams of fuel and oxidizer which are generated by the vaporization of each solid component. The reaction zone, centered above the interfacial region, is called the "phalanx" which leads the hot reaction gases through the unburned solid. Figure 11 shows the "phalanx" flame at steady state. The greatest heat flux from the reaction zone occurs in the vicinity of the interface between the two solid phases and solid component vaporization occurs most rapidly near the interface. Fenn assumed that the burning rate of the propellant is the rate at which this "phalanx" reaction zone proceeds into the propellant.

Sturm proposed that the "phalanx" flame follows its penetration course along the interface between the fuel and oxidizer and may proceed all the way around a small oxidizer crystal before the crystal is completely consumed. The AP crystal would then become separated

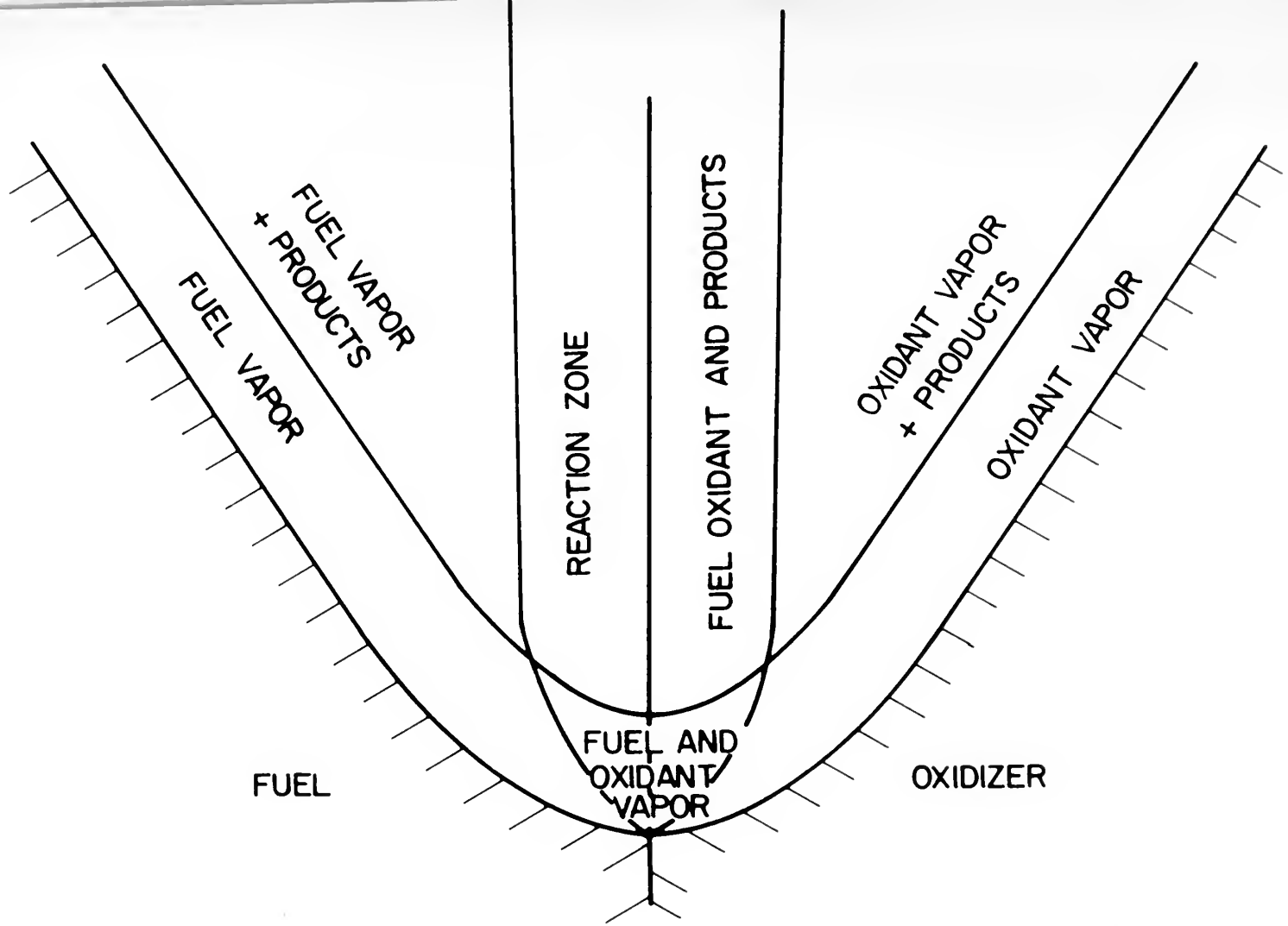

FIGURE 11 . PHALANX FLAME AT STEADY STATE .(TAKEN FROM REFERENCE 10)

from the fuel matrix by a layer of gases. If the AP crystals are very small, the drag forces produced by the normal gas flow from the gasifying surfaces may force these crystals away from the propellant surface. These AP crystals on or near the burning surface of the propellant would thus be removed. This effect causes an AP crystal depletion on or near the surface and a corresponding reduction in burning rate. In higher than 0g conditions, the acceleration force holds these small AP crystals on the surface and increases the burning rate. A given AP crystal is considered to remain in the neighborhood of the surface until decomposition reduces its size enough for the drag force to become greater than the acceleration force. This AP crystal size was called the critical particle size and was determined by Sturm as follows:

The acceleration force on a particle is given by

$$F_g = \frac{\pi d^3 \rho_d a}{6} \tag{4}$$

where

d = particle diameter (cm)

ρ_d = particle density (gm/cm^3)

a = acceleration (cm/sec^2)

Assuming stokes flow, the drag force on a spherical particle is given by

$$F_D = 3\pi \mu_g d V_g \tag{5}$$

where

μ_g = gas phase viscosity (gm/cm sec)

V_g = gas phase velocity (cm/sec)

Equating F_g to F_D yields the critical particle size. Thus

$$d_{critical} = \left[\frac{18 \mu_g V_g}{\rho_d a} \right]^{\frac{1}{2}} \quad (6)$$

From continuity

$$\rho_g A_g V_g = \rho_p A_p V_p \quad (7)$$

where

A_g = gas flow area (cm^2)

A_p = propellant burn area (cm^2)

V_p = propellant burning rate (cm/sec)

ρ_p = propellant density (gm/cm^3)

For propellant strands enclosed in rigid inhibitors, $A_p = A_g$ and $V_p = \dot{r}$ and Equation 4 becomes

$$V_g = \frac{\rho_p \dot{r}}{\rho_g} \quad (8)$$

Substituting Equation 8 into Equation 6 yields

$$d_{critical} = \left[\frac{18 \mu_g \rho_p \dot{r}}{\rho_g \rho_d a} \right]^{\frac{1}{2}} \quad (9)$$

Assuming a perfect gas,

$$\rho_g = \frac{p}{R_g T_g} \quad (10)$$

Substituting Equation 10 into Equation 9 yields

$$d_{critical} = \left[\frac{18 \mu_g \rho_p \dot{r} R T_g}{p \rho_d a} \right]^{\frac{1}{2}} \quad (11)$$

Using representative values for nonmetallized composite propellants, Sturm has estimated the critical particle size at two pressures to be

$$d_{critical_{500}} = 152 \left[\frac{1}{G}\right]^{\frac{1}{2}} \quad \text{microns} \tag{12}$$

$$d_{critical_{1000}} = 108 \left[\frac{1}{G}\right]^{\frac{1}{2}} \quad \text{microns} \tag{13}$$

where

$G = a/g$

g = standard acceleration due to gravity.

It is observed from Equation 11, that for a given propellant

$$d_{critical} \propto \left[\frac{\dot{r}}{pa}\right]^{\frac{1}{2}} \tag{14}$$

B. ANALYTICAL MODEL

Allowing for the increased heat transfer to the surface due to the retention of AP crystals on the surface, Sturm has proposed the following equation for burning rate augmentation

$$\frac{\dot{r}}{\dot{r}_o} = \frac{1}{1 - \frac{w_o f h_c J}{h_v}} \tag{15}$$

where

w_o = mass fraction of small size AP oxidizer in the propellant

f = fraction of the combustion energy release transferred to the propellant surface

h_c = energy released by combustion of AP oxidizer particles

h_v = energy required to heat up and vaporize a unit mass of propellant

J = fraction of small AP oxidizer particle mass released by decomposition on the propellant surface.

As noted by Sturm, the main limitation to the model is that f, h_c, J, and h_v are unknown functions of acceleration and pressure. J varies with acceleration through $d_{critical}$. Practical application of the model is therefore limited. Sturm's model does, however, allow the prediction of various qualitative effects.

Using Equation 15 Sturm has predicted that:

1) Burning rate augmentation is not a function of G <u>until</u> the acceleration level is sufficient to hold the largest AP crystal of the smaller AP crystal distribution (in a bi-modal mix) on the propellant surface.

2) Augmentation increases with G and reaches a limiting value when all of the small AP crystals are held on the surface.

3) Augmentation increases with increasing pressure at a given G.

4) Augmentation increases with decreasing base burning rate.

5) Augmentation increases with increasing weight percentage of small AP oxidizer crystals.

6) Augmentation increases with increasing initial propellant temperature at high G.

Sturm found qualitative agreement between the model and his experimental results.

V. EXPERIMENTAL RESULTS AND DISCUSSION

A. GENERAL DISCUSSION

The experimental results and discussion are arranged into five sections. The first presents the effect of pressure on burning rate augmentation for two propellants, namely, N-1 and N-3. The second section presents the effect of AP size and base burning rate on burning rate augmentation at 500 psia. In order to obtain these combined effects, propellants N-1, N-2, and N-3 were utilized as they all had different AP sizes and different base burning rates. The third section presents the effect of the base burning rate on burning rate augmentation at 500 psia. This effect was obtained by utilizing propellants N-2, N-4, and N-5, which had the same AP size, but different base burning rates. The fourth section presents the effect of AP size on burning rate augmentation at 500 psia. This effect was obtained by utilizing propellants N-1 and N-4 which have approximately the same base burning rate, but a different AP size. The last section will compare the experimental results with the model proposed by Sturm.

The data are presented as either the absolute burning rate, in inches/second, versus acceleration or the burning rate augmentation versus acceleration. The burning rate augmentation is defined as the burning rate at a given acceleration and pressure divided by the burning rate of the propellant with the centrifuge at rest. The centrifuge at rest is defined as the 0g burning rate or base burning rate condition. The base burning rate was obtained by averaging the

data from several 0g runs. Runs were made at 0g, 50g, 100g, 150g, 250g, 500g and 1000g in order to obtain the data points.

During all discussions of results, it will be convenient to assume that the physical model proposed by Sturm for the effects of acceleration on nonmetallized AP propellant is correct. This is of no consequence because the data reported herein confirm the basic physical model proposed by Sturm.

During all experimental runs, the propellant was subjected to an acceleration field normal and into the burning surface. All of the data obtained are presented in Tables II - VI. The augmentation and burning rates are given to three (3) significant figures. A maximum possible error of two (2) per cent in the burning rate would cause a maximum possible error of four (4) per cent in the augmentation.

The curves drawn on Figures 12-19 indicate the trend of data and not quantitative burning rate data.

TABLE II

DATA FOR PROPELLANT N-1

Length (inches)	Burning Rate (in/sec)	$\dot{r}/\dot{r}_o$	G	Average Bomb Pressure (psia)
2.008	.371	-	0	486
2.015	.371	-	0	487
2.010	.378	1.02	50	481
2.010	.373	1.01	50	484
2.025	.379	1.02	50	483
1.984	.371	1.00	100	481
2.010	.393	1.06	100	480
2.014	.384	1.04	99	482
2.008	.379	1.02	149	481
1.995	.410	1.11	149	480
2.006	.379	1.02	149	481
2.003	.413	1.11	251	482
2.007	.394	1.06	249	481
2.022	.388	1.05	247	480
2.000	.426	1.15	501	479
2.006	.405	1.09	501	478
2.007	.427	1.15	1000	477
2.008	.419	1.13	1000	476
2.010	.483	-	0	997
2.005	.472	-	0	982
2.019	.476	1.00	50	977

TABLE II (Continued)

DATA FOR PROPELLANT N-1

Length (inches)	Burning Rate (in/sec)	$\dot{r}/\dot{r}_o$	G	Average Bomb Pressure (psia)
2.015	.478	1.00	100	978
2.013	.490	1.03	149	982
2.012	.537	1.12	251	981
1.998	.577	1.21	501	987
2.002	.659	1.38	996	994
2.002	.676	1.42	996	988

TABLE III

DATA FOR PROPELLANT N-2

Length (inches)	Burning Rate (in/sec)	$\dot{r}/\dot{r}_o$	G	Average Bomb Pressure (psia)
2.022	.266	-	0	491
2.022	.257	-	0	490
2.009	.266	1.02	50	489
2.028	.257	.98	50	486
2.006	.297	1.14	101	487
2.013	.274	1.05	100	487
2.001	.320	1.22	149	488
2.026	.306	1.17	148	487
2.012	.290	1.11	151	486
2.019	.331	1.27	249	488
2.025	.309	1.18	249	488
2.021	.307	1.17	249	486
2.014	.346	1.32	504	485
2.028	.344	1.32	501	485
2.020	.360	1.38	1000	484
2.010	.350	1.34	1000	482

TABLE IV

DATA FOR PROPELLANT N-3

Length (inches)	Burning Rate (in/sec)	$\dot{r}/\dot{r}_o$	G	Average Bomb Pressure (psia)
1.753	.164	-	0	493
2.000	.162	-	0	494
1.998	.161	-	0	492
1.757	.165	1.02	52	494
1.827	.166	1.02	50	496
1.993	.163	1.00	52	490
2.018	.179	1.10	100	493
2.030	.174	1.07	101	496
2.002	.172	1.06	101	489
2.014	.175	1.08	149	487
2.019	.179	1.10	149	493
1.991	.167	1.03	149	488
2.022	.174	1.07	249	491
1.996	.168	1.04	251	492
1.997	.171	1.05	251	486
2.012	.178	1.10	501	477
1.897	.153	.94	499	482
2.000	.151	.93	501	483
2.004	.167	1.03	551	483
2.000	.144	.89	606	482
2.006	.228	-	0	1002

TABLE IV (Continued)

DATA FOR PROPELLANT N-3

Length (inches)	Burning Rate (in/sec)	$\dot{r}/\dot{r}_o$	G	Average Bomb Pressure (psia)
2.021	.228	1.00	50	996
2.020	.252	1.11	100	997
2.008	.264	1.16	149	1000
1.752	.273	1.20	251	998
2.003	.266	1.17	501	996
2.010	.245	1.07	1000	991

TABLE V

DATA FOR PROPELLANT N-4

Length (inches)	Burning Rate (in/sec)	$\dot{r}/\dot{r}_o$	G	Average Bomb Pressure (psia)
2.012	.427	-	0	485
2.025	.431	-	0	483
2.012	.439	1.02	51	476
1.772	.473	1.10	49	469
1.995	.446	1.04	51	473
1.991	.484	1.13	100	474
1.992	.425	.99	100	471
1.992	.464	1.08	100	471
2.001	.441	1.03	99	475
1.982	.413	.96	149	471
1.992	.415	.97	149	466
2.001	.433	1.01	148	468
2.001	.465	1.08	249	472
1.995	.487	1.14	249	468
1.999	.471	1.10	251	468
2.004	.456	1.06	499	470
2.000	.447	1.04	504	462
2.002	.442	1.03	1000	465
1.999	.423	.99	1000	463
1.999	.471	1.10	1000	463

TABLE VI

DATA FOR PROPELLANT N-5

Length (inches)	Burning Rate (in/sec)	$\dot{r}/\dot{r}_o$	G	Average Bomb Pressure (psia)
2.018	.467	-	0	484
2.023	.444	-	0	483
2.020	.421	-	0	476
2.003	.417	-	0	484
1.845	.499	1.14	50	476
2.004	.421	.96	53	477
2.024	.420	.96	100	475
2.002	.426	.97	100	479
2.020	.476	1.09	149	477
2.004	.466	1.07	148	479
2.021	.480	1.10	251	476
1.998	.465	1.06	251	479
2.010	.458	1.05	504	473
2.021	.488	1.12	501	474
2.005	.445	1.02	499	474
2.008	.455	1.04	501	476
2.007	.455	1.04	1000	472
2.005	.457	1.05	1000	471
2.004	.434	.99	1004	472

B. EFFECT OF PRESSURE ON AUGMENTATION

Two nonmetallized composite propellants, N-1 and N-3, were investigated at pressures of 500 and 1000 psia. Plots of burning rate augmentation versus acceleration for each of these propellants are presented in Figures 12 and 13. The data presented in these figures indicate that each of the propellants exhibited an increase in burning rate with acceleration except at low acceleration.

At a pressure of 500 psia, propellant N-1 exhibited a gradual burning rate increase as the acceleration field was increased. At 1000g the augmentation was 14 per cent. At a pressure of 1000 psia, propellant N-1 exhibited no change in burning rate augmentation up to 100g and then a pronounced increase up to a value of 40 per cent at 1000g. From 0g to about 250g there was no appreciable difference in the burning rate augmentation between tests conducted at 500 psia and 1000 psia for N-1.

At a pressure of 500 psia, propellant N-3 exhibited a burning rate augmentation of 7.5 per cent at about 150g. The augmentation then decreased to 6 per cent at 250g. From 250g to 606g the data became unreliable due to the random time interval from ignition of the black powder until the propellant commenced to burn in a steady manner. Propellant N-3 at 500 psia would not continue to burn after ignition above 606g. At a pressure of 1000 psia, propellant N-3 exhibited no burning rate augmentation from 0g to 50g and then a pronounced increase up to a value of 20 per cent at 250g. Any further increase in acceleration produced unreliable data due to reason mentioned previously. Propellant N-3 at 1000 psia did, however, ignite and burn up to and including 1000g. From 0g to about 75g there was no appreciable difference in the burning rate augmentation.

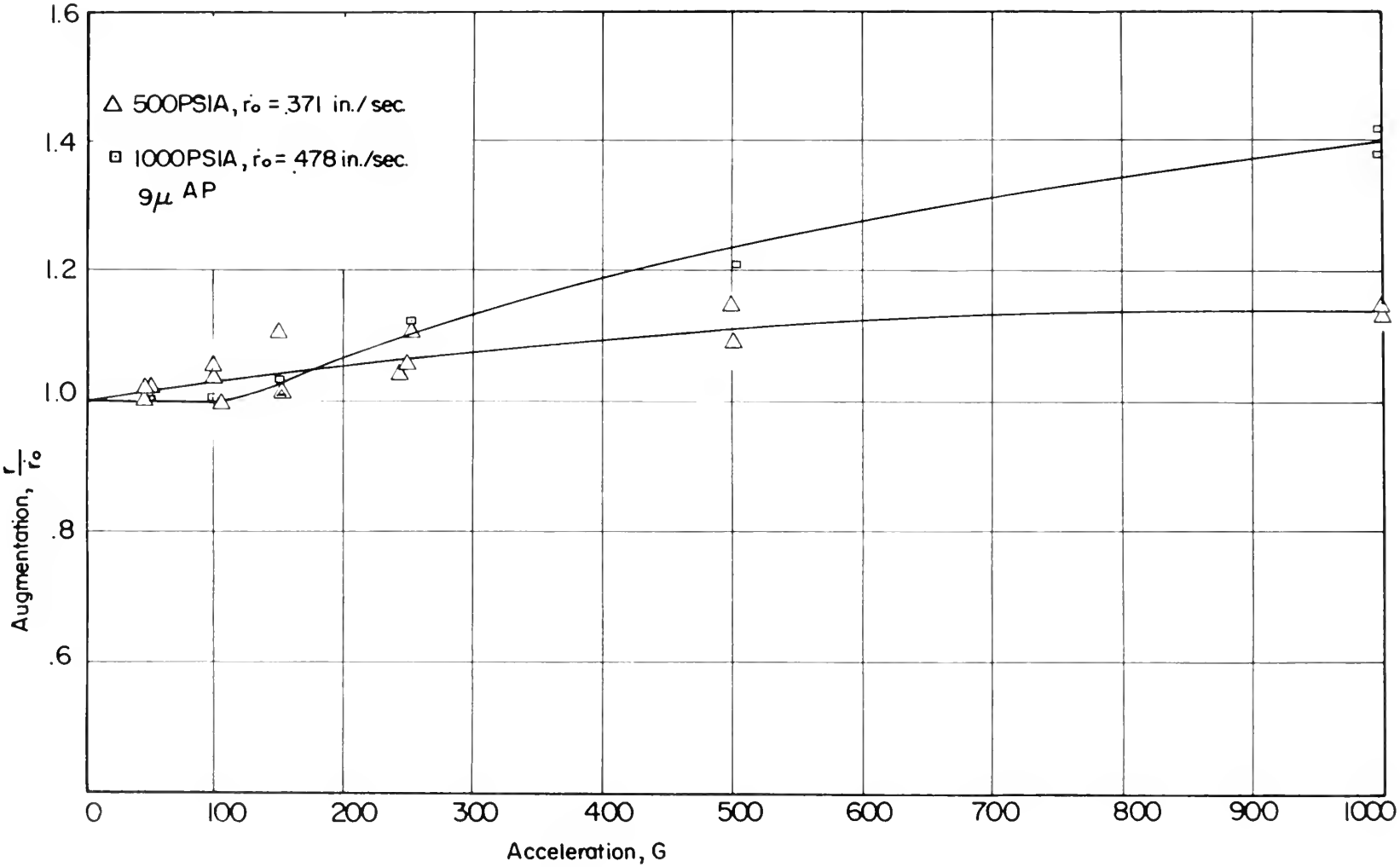

FIGURE 12. EFFECT OF PRESSURE ON BURNING RATE AUGMENTATION OF NON-METALLIZED COMPOSITE PROPELLANT (N-1)

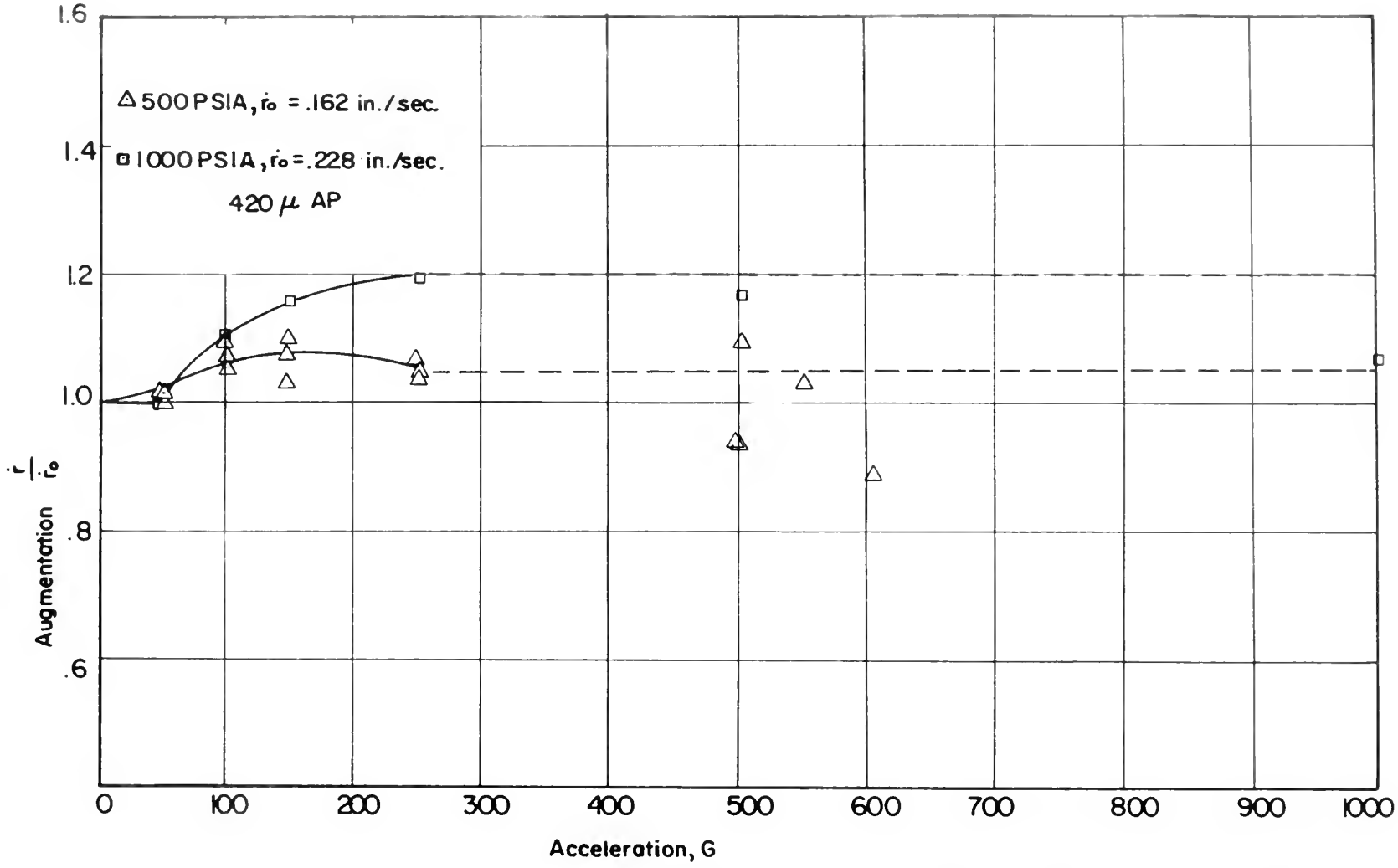

FIGURE 13. EFFECT OF PRESSURE ON BURNING RATE AUGMENTATION OF NON-METALLIZED COMPOSITE PROPELLANT (N-3)

The data from propellants N-1 and N-3 indicate that except at low accelerations, increasing the pressure increases the acceleration sensitivity. Referring to Sturm's physical model for nonmetallized propellants, an explanation of the observed behavior for propellants N-1 and N-3 can be made. As mentioned earlier, Fenn has shown that the penetration rate of the "phalanx" flame increases with increasing pressure. At 500 psia the penetration rate is probably low enough that the "phalanx" flame does not burn all the way around some of the AP crystals before they are completely consumed. Therefore they do not become detached from the PBAN. At 0g some AP crystals are detached; however, as the acceleration level is increased they are held on the surface. This gradually increased the burning rate augmentation. At 1000 psia the penetration rate is higher and more AP crystals are being freed to leave the surface at 0g. As the acceleration level is increased there is little or no effect on burning rate augmentation until the acceleration level becomes great enough to begin holding some AP crystals on the surface. As the acceleration is increased above this threshold, the augmentation increases at a pronounced rate.

Thus, increasing the pressure level resulted in: 1) apparent commencement of burning rate augmentation at higher acceleration levels although possible error and data scatter preclude a definite conclusion; 2) achievement of the maximum burning rate augmentation at a higher acceleration level; and 3) a higher value of burning rate augmentation except at low accelerations.

One possible explanation is presented to explain the failure of propellant N-3 to ignite above approximately 600g at 500 psia and

for the successful ignition at all accelerations to 1000g at 1000 psia. The AP crystals are denser than the binder. At 500 psia and high accelerations, the large AP crystals (420μ) are forced into the somewhat compressible binder. This provides a fuel rich surface which either ignites erratically or not at all. As the pressure is increased to 1000 psia, the binder becomes less compressible. The acceleration force cannot then force the AP crystals as far into the binder before ignition. It still might burn erratically. Propellant N-1 had smaller AP crystals than N-3 and therefore there was always enough oxidizer on the surface to allow ignition. After the failure of propellant N-3 to ignite at 500 psia at high G loads, the same propellant strand was then fired successfully at 0g and 500 psia. This precluded the possibility of defectively manufactured propellant.

C. EFFECT OF AP SIZE AND BASE BURNING RATES ON AUGMENTATION.

When the AP crystal size is increased the 0g burning rate decreases. This is a result of the larger AP crystals having less surface area available to react with the binder. Thus, burning rate augmentation may be affected by both parameters as the AP size is changed. Propellants N-1, N-2, and N-3 had different AP crystal sizes and base burning rates. Figure 14 is a plot of burning rate versus acceleration for the three propellants. Figure 15 shows the combined effect of AP size and base burning rate on the burning rate augmentation at 500 psia for propellants N-1, N-2, and N-3. The data for N-3 is inconclusive. Propellant N-2 exhibits a pronounced increase in augmentation above approximately 50g to a maximum of 37 per cent augmentation at 1000g. N-1 exhibits a gradual increase in burning rate augmentation with an increase in acceleration level to a maximum of 14 per cent at 1000g.

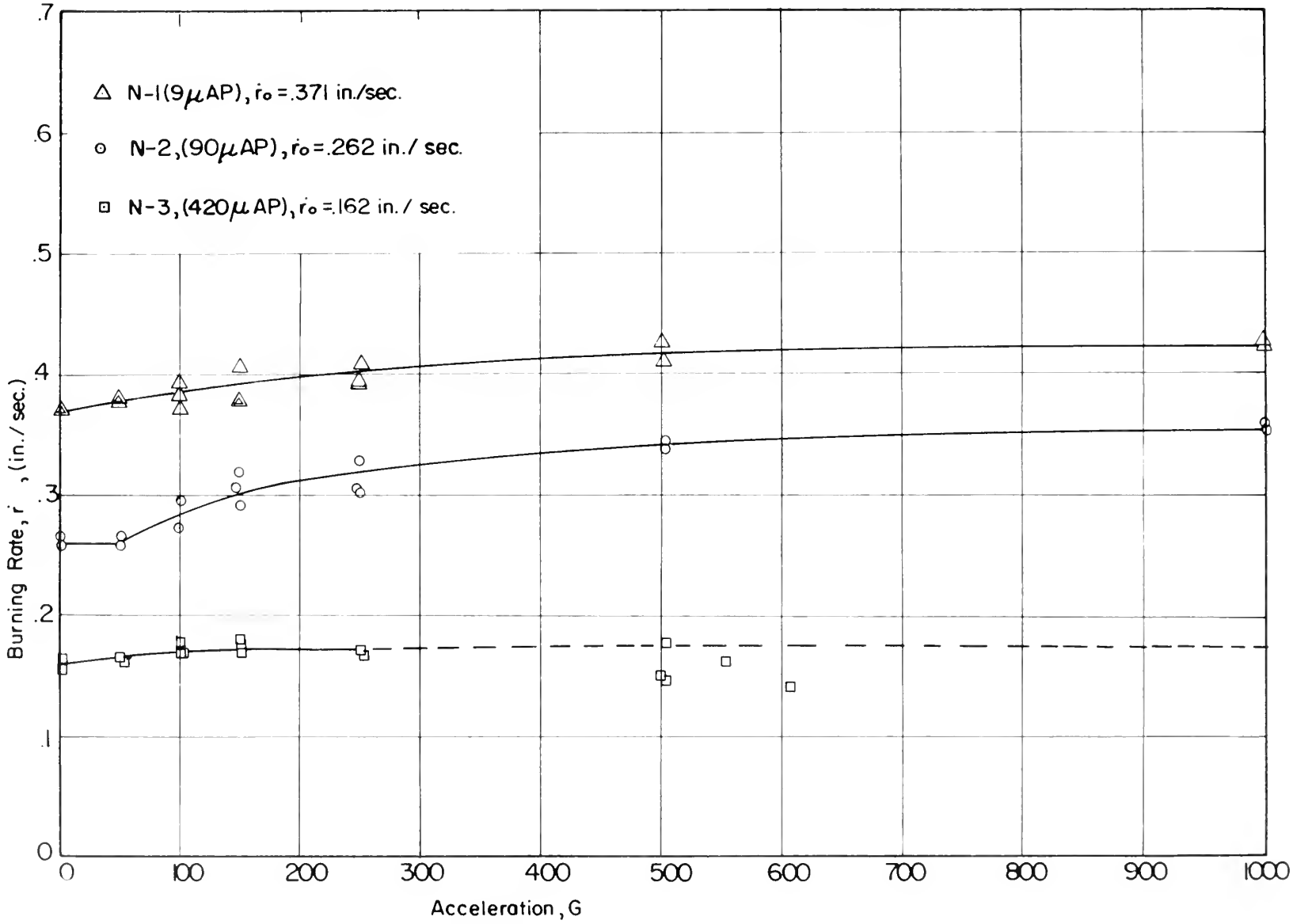

FIGURE 14. EFFECT OF AP SIZE AND $\dot{r}_o$ ON BURNING RATE OF NON-METALLIZED COMPOSITE PROPELLANTS AT 500 PSIA

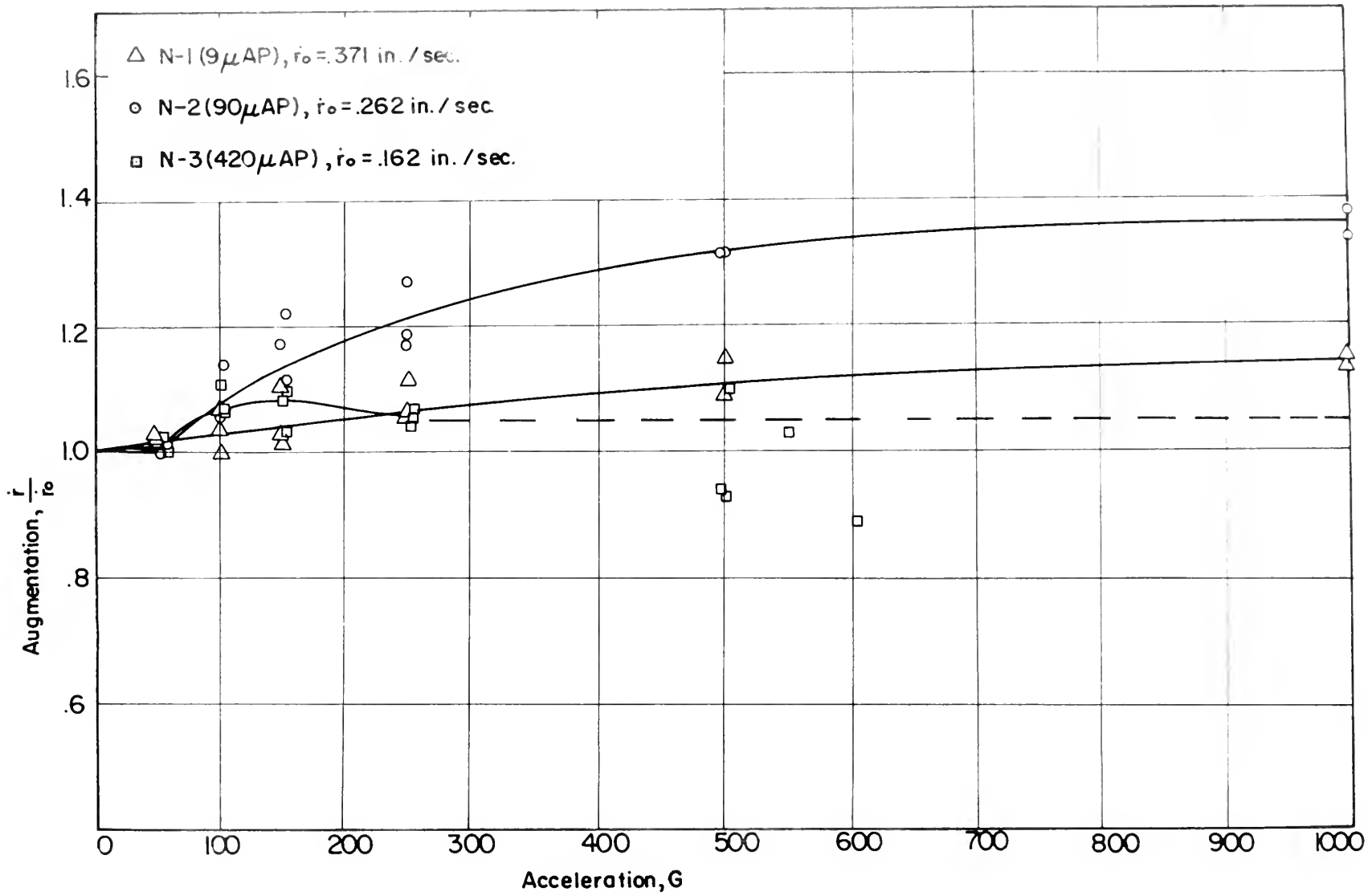

FIGURE 15. EFFECT OF AP SIZE AND $\dot{r}_o$ ON BURNING RATE AUGMENTATION OF NON-METALLIZED COMPOSITE PROPELLANTS AT 500 PSIA.

N-1 had a small AP crystal size (9μ) and a high base burning rate. Thus many AP crystals leave the surface at 0g. As the acceleration level is increased, more and more AP crystals are held on the surface and the burning rate augmentation increases slightly.

N-2 had a mean AP crystal size of 90μ. The size distribution presented previously indicates that some crystals existed with diameters as small as 40μ. The base burning rate of propellant N-2 was also less than that of propellant N-1.

The smallest AP crystals in propellant N-3 were 420μ. Very few AP crystals leave the surface at 0g. Burning rate augmentation should be small and increase to its maximum at low acceleration since it doesn't take a significant acceleration to hold all the AP crystals on the surface.

In the next two sections, the separate effects of AP size and base burning rate on augmentation will be examined.

D. EFFECT OF BASE BURNING RATE ON AUGMENTATION

A plot of burning rate versus acceleration for propellants N-2, N-4, and N-5 is shown in Figure 16. Figure 17 shows the effects of base burning rate on the burning rate augmentation at 500 psia. Propellants N-2, N-4, and N-5 had the same AP size (90μ), but different base burning rates due to the addition of a catalyst in propellant N-4 (1% Fe_2O_3) and propellant N-5 (2% Fe_2O_3). Propellants N-4 and N-5 exhibited erratic augmentation below 250g with only 4 per cent augmentation at 1000g. N-2 exhibited little augmentation below 50g and then a pronounced augmentation to a maximum of 36 per cent at 1000g.

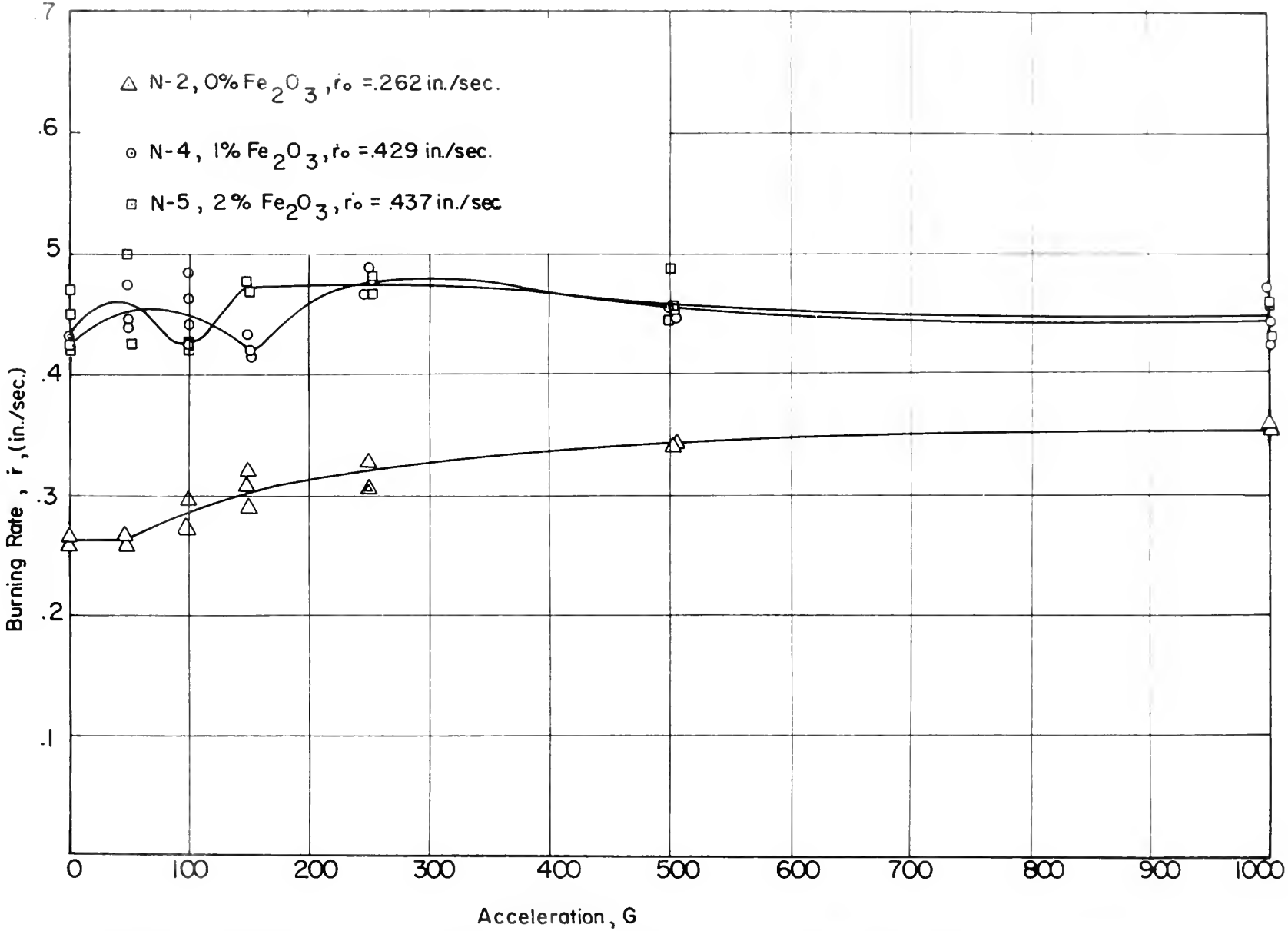

FIGURE 16. EFFECT OF $\dot{r}_o$ ON BURNING RATE OF NON-METALLIZED COMPOSITE PROPELLANTS AT 500PSIA (90 μ AP)

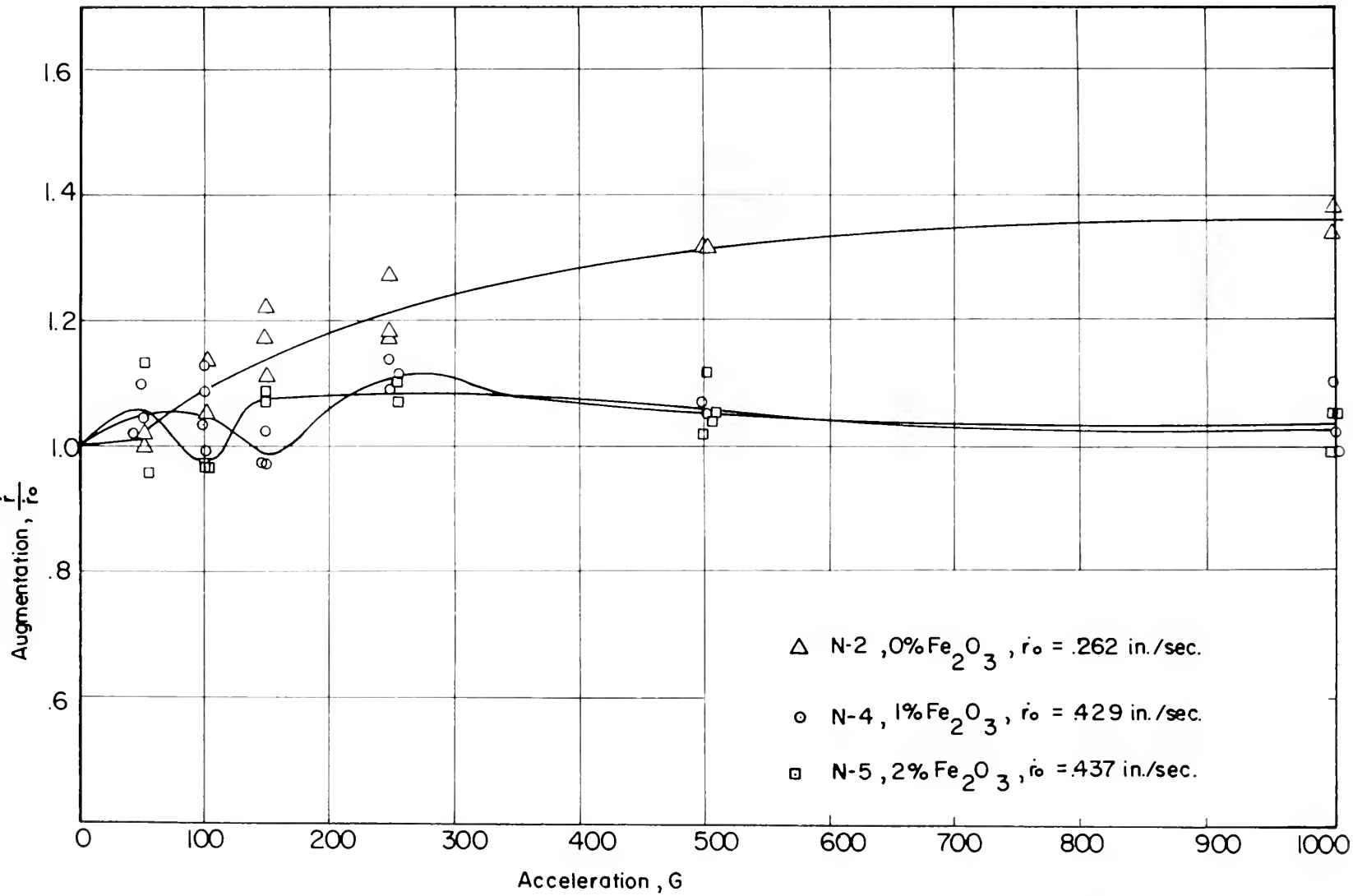

FIGURE 17. EFFECT OF $\dot{r}_o$ ON BURNING RATE AUGMENTATION OF NON-METALLIZED COMPOSITE PROPELLANTS AT 500 PSIA. (90 μ AP)

Propellant N-2 had the lower base burning rate. Less AP crystals will leave the surface at 0g than for propellants N-4 or N-5. The ones that do leave the surface will also have a lower velocity than for propellants N-4 or N-5. Therefore for propellant N-2, a lower acceleration is required to hold the AP crystals on the surface and higher burning rate augmentation is obtained. Propellants N-4 and N-5 had AP crystals leaving the surface with a very high velocity, and the acceleration forces are not large enough to hold a significant number of AP crystals on the surface to obtain any consequential burning rate augmentation.

The yellow iron-oxide had a mean diameter less than 0.5μ and therefore the acceleration and drag forces were insignificant to 1000g.

E. EFFECT OF AP SIZE ON AUGMENTATION

A plot of burning rate versus acceleration for propellants N-1 and N-4 is shown in Figure 18. Figure 19 shows the effects of AP size on burning rate augmentation at 500 psia. It was attempted to formulate propellant N-4 so that it had a closer base burning rate to propellant N-1 and therefore have only AP size as the variable. The difference in base burning rates is approximately 16 per cent and this difference is considered in the following discussion. Propellant N-4 exhibited significant data scatter below approximately 150g with only a 4 per cent augmentation at 1000g. Propellant N-1 exhibited a gradual increase in augmentation with increase in acceleration to a value of 14 per cent at 1000g.

Propellant N-1 had the smaller AP size and many of the AP crystals will leave the surface at 0g. As the acceleration level is increased,

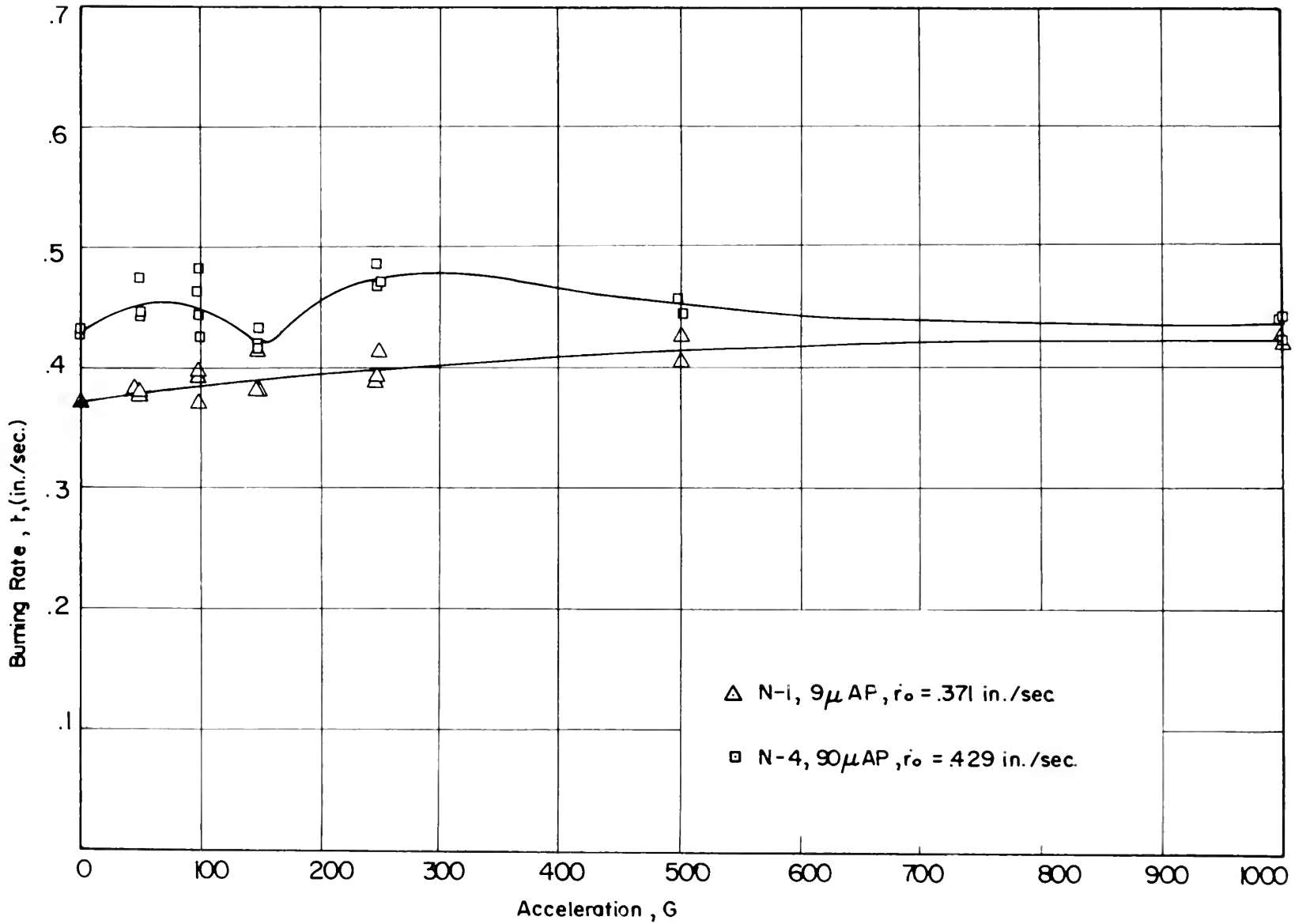

FIGURE 18 . EFFECT OF AP SIZE ON BURNING RATE OF NON-METALLIZED COMPOSITE PROPELLANTS AT 500 PSIA.

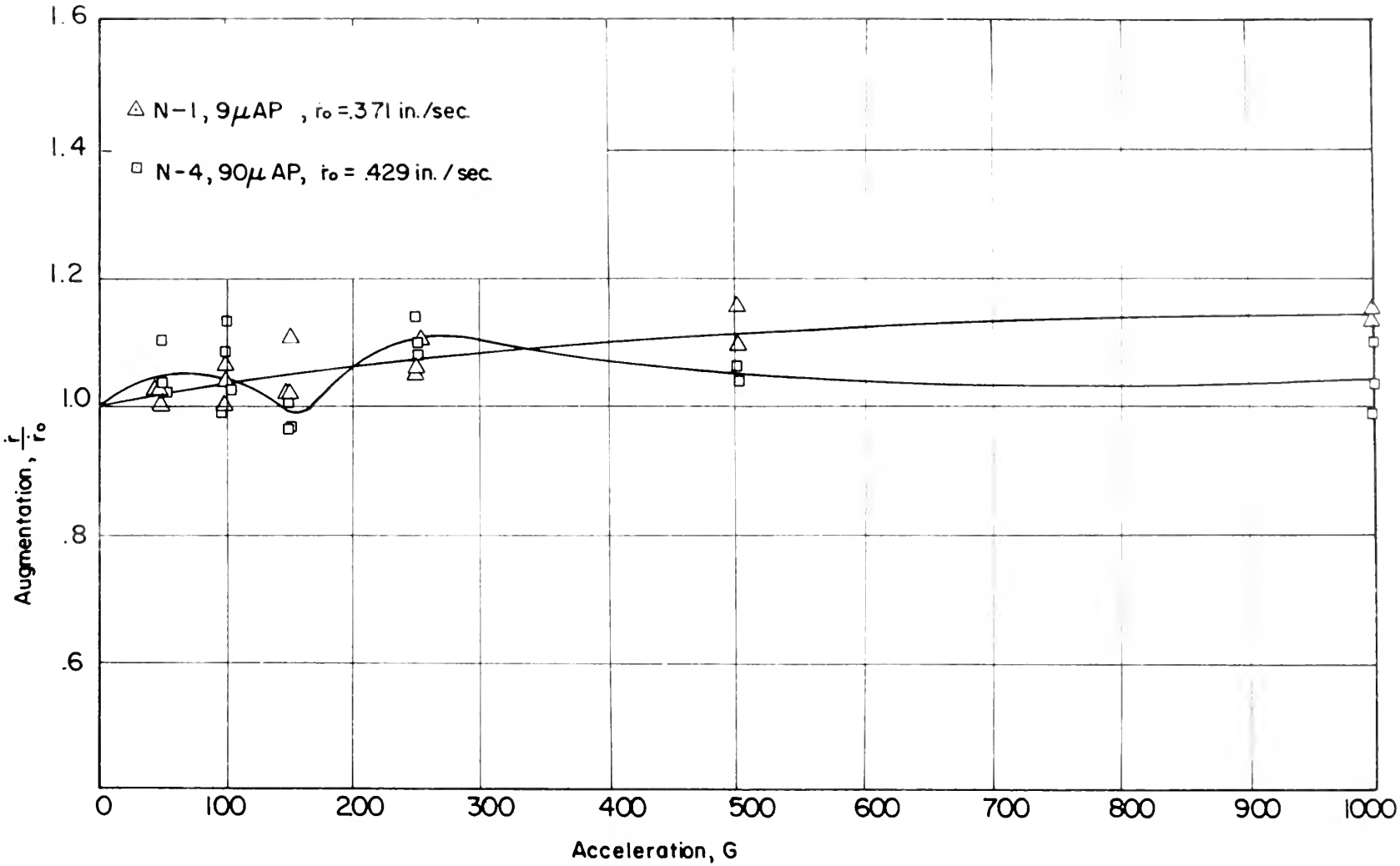

FIGURE 19. EFFECT OF AP SIZE ON BURNING RATE AUGMENTATION OF NON-METALLIZED COMPOSITE PROPELLANTS AT 500 PSIA.

more and more AP crystals are held on the surface and therefore augmentation will gradually increase. N-4 had a larger AP size and a slightly larger base burning rate. As stated earlier, the mass distribution includes AP crystals to 40μ. At 0g these smaller AP crystals are probably leaving the surface and as the acceleration level is increased they are held on the surface, thereby causing augmentation.

Since the base burning rates are not exactly the same, the two effects of AP size and base burning must be further analyzed. Referring to Figure 15, it is observed that in comparing the data of propellant N-2 and propellant N-1 at 1000g, a 23 per cent increase in augmentation was accomplished by a 29 per cent decrease in the base burning rate and a 1000 per cent increase in AP size. Referring to Figure 19, it is observed that in comparing the data of propellant N-1 and propellant N-4 at 1000g, a 10 per cent increase in augmentation was accomplished by a 14 per cent decrease in base burning rate and a 1000 per cent decrease in AP size. Referring to Figure 17, it can be seen that in comparing propellant N-2 with propellant N-4 at 1000g, a 32 per cent increase in augmentation was accomplished by a 39 per cent decrease in base burning rate with AP size constant. These relations show that the augmentation is almost entirely dependent on base burning rate at high accelerations and that AP crystal size has little effect.

F. COMPARISON OF THE DATA WITH STURM'S MODEL

The data obtained in the investigation leads to the following effects which are in accord with Sturm's analytical model:

1. Augmentation is not a function of G until the acceleration level is sufficient to hold the largest AP crystal size of the smaller AP crystal distribution on the propellant surface.

2. Augmentation increases with G and reaches a limiting value when all of the small AP is held on the surface.

3. Augmentation increases with decreasing nominal burning rate.

Since unimodal AP crystals were used in the investigation, the effect of the weight percentage of small AP crystals was not investigated. No experiments were attempted at any temperature other than room temperature so there is no comparison with Sturm's sixth prediction which was presented above.

Stokes' drag law is valid for spheres with no mass flux from the surface and low Reynolds numbers ($R_e < 1$). The small AP oxidizer particles are not true spheres, have a mass flux out of their surface since they are decomposing, and the Reynolds numbers encountered may be significantly greater than one. Sturm assumed Stokes' flow around the AP crystals which had become separated from the binder by the "phalanx" flame. This assumption produced a critical particle size with dependence on burning rate, pressure, and acceleration as given by Equation (14) and repeated below:

$$d_{critical} \propto \left[\frac{\dot{r}}{pa}\right]^{\frac{1}{2}} \tag{14}$$

which indicates a $\frac{1}{2}$ power dependence of critical particle size on burning rate.

The Reynolds number is

$$R_e = \frac{V_g \, d\rho_g}{\mu_g} = \frac{\dot{r} d \, \rho_p}{\mu_g} \tag{16}$$

The smallest AP crystal size used in this experiment was 9μ and the lowest burning rate was .162 in/sec. Using these quantities together with

$$\rho_p = 1.65 \text{ gm/cm}^3$$

$$\mu_g = 6 \times 10^{-4} \text{ gm/cm sec}$$

yields a minimum expected Reynolds number of approximately six. The AP crystals are not spherical and their surface is undergoing reactions which emit gases. However, the above expected minimum Reynolds number indicates that the Stokes' flow assumption may be invalid.

The standard drag equation for $R_e > 1.0$ [11] is

$$F_d = \frac{\pi}{8} C_D \rho_g d^2 V_g^2 \tag{17}$$

where

C_D = Drag coefficient

Therefore for $R_e > 1.0$

$$F_d \propto \frac{d^2 \dot{r}^2}{p} \tag{18}$$

and

$$d_{critical} = \frac{3 C_D \rho_p^2 \dot{r}^2 R_g T_g}{pa \rho_d} \tag{19}$$

or

$$d_{critical} \propto \frac{\dot{r}^2}{pa} \tag{20}$$

For inert spheres in steady flow, a Reynolds number of 100 and the corresponding drag coefficient of approximately 1.0 results in a $d_{critical}$ versus G curve which closely approximates the $d_{critical}$ versus G curve for Stokes' flow.

Using the same procedures employed by Sturm [2], but using Equation 20 instead of Equation 14 , the non-Stokes' theory was compared with the experimental data from two of Sturm's nonmetallized propellants. These comparisons together with the Stokes' flow model results are depicted by Figures 20 and 21. It can be observed from these figures that Equation 20 for $d_{critical}$ more nearly agrees with Sturm's experimental data at low acceleration levels than Equation 14 . At the higher acceleration levels there is no appreciable difference.

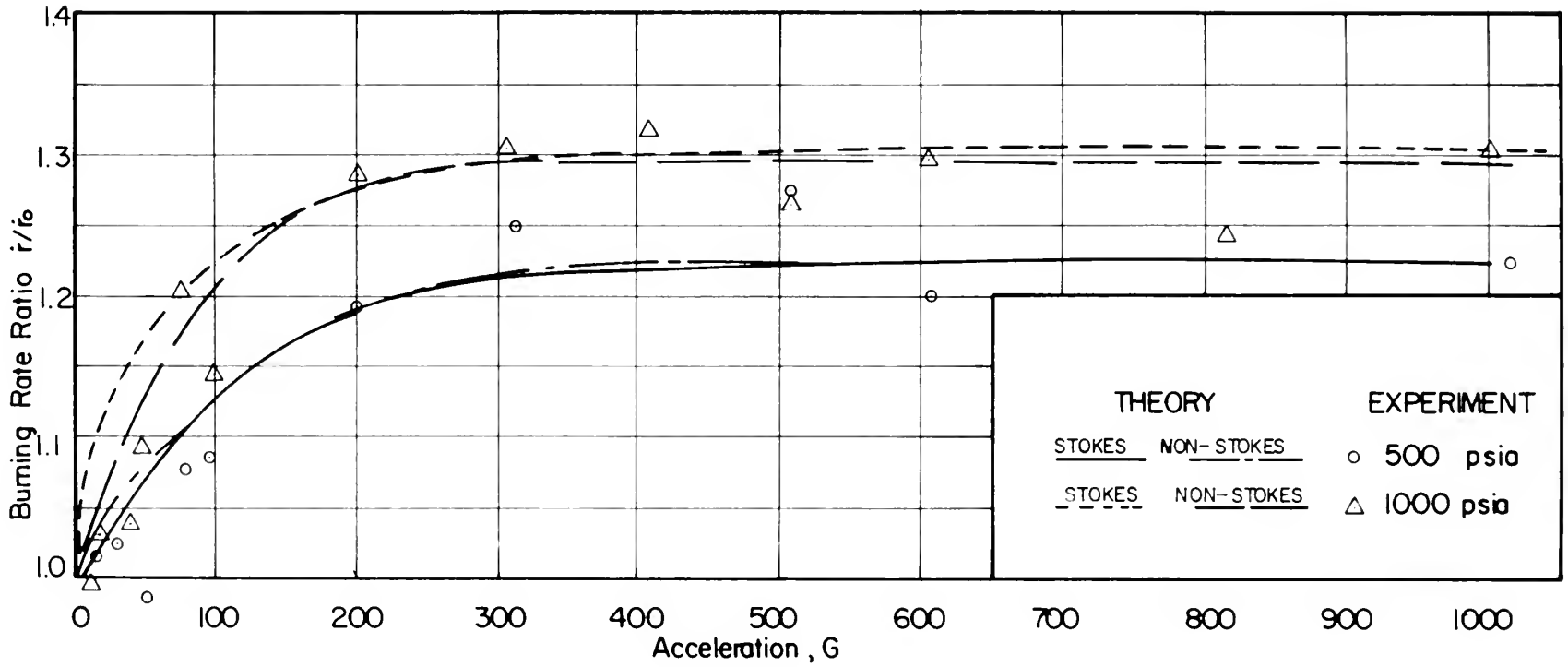

FIGURE 20. COMPARISON OF STOKES VS. NON-STOKES THEORY WITH EXPERIMENT FOR P 410 PROPELLANT (Adapted From Reference 2)

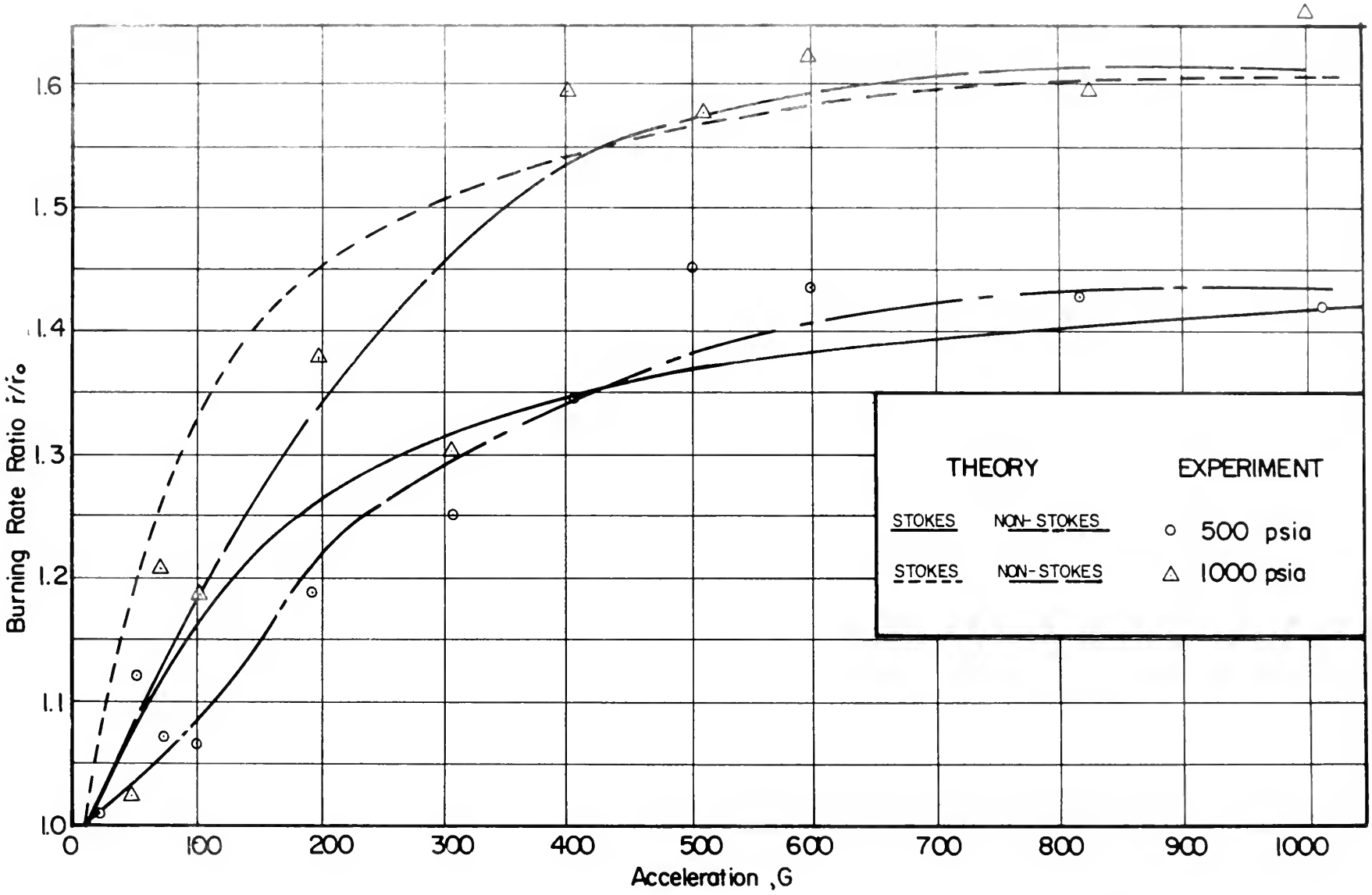

FIGURE 21 COMPARISON OF STOKES VS. NON-STOKES THEORY WITH EXPERIMENT FOR P 411 PROPELLANT (Adapted From Reference 2)

VI. CONCLUSIONS

The conclusions derived from this investigation can be summarized as follows: First, augmentation is not a function of acceleration until the acceleration level is sufficient to hold the larger of the AP crystals, which are forced from the surface at 0g, on the propellant surface. Second, augmentation increases with acceleration and reaches a limiting value when all the AP crystals are held on the surface. Third, augmentation increases with decreasing base burning rate. Fourth, augmentation increases with increasing pressure except at low accelerations. Fifth, increasing pressure resulted in achievement of the maximum burning rate augmentation at a higher acceleration level. Sixth, augmentation has a strong dependence on base burning rate and a weak dependence on AP crystal size.

It was found that Sturm's physical model successfully correlated the experimental results. The experimental results also compare favorably with Sturm's analytical model. However, the dependence of $d_{critical}$ on $\frac{\dot{r}^2}{pa}$ appears to better correlate with experimental data at low accelerations than does $d_{critical}$ based on Stokes' flow.

REFERENCES

1. Naval Postgraduate Report Number NPS-57RV7071A, An Investigation of the Effect of Acceleration on the Burning Rate of Composite Propellants, by J. E. Anderson and R. E. Reichenbach, July 1967.

2. Sturm, E. J., A Study of the Burning Rates of Composite Propellants in Acceleration Fields, Ph.D. Thesis, Naval Postgraduate School, Monterey, 1968.

3. Naval Postgraduate School Technical Report NPS-57RV8121A, A Study of the Burning Rates of Composite Solid Propellants in Acceleration Fields, by E. J. Sturm and R. E. Reichenbach, 5 December 1968.

4. UTC Report Number UTC 2281-FR, Investigation of Internal Ballistic Effects in Spinning Solid Propellant Motors, by P. G. Willoughby, C. T. Crowe, R. Dunlap, and K. L. Baker, October 1968.

5. Northam, G. B. and Lucy, M. H., On the Effects of Acceleration Upon Solid Rocket Performance, paper presented at 1968 ICRPG/AIAA 3rd Solid Propulsion Conference, Atlantic City, New Jersey, 4-6 June 1968.

6. Department of Aeronautics Technical Note 66T-4, 76-Inch Diameter Centrifuge Facility, by J. Anderson and R. Reichenbach, September 1966.

7. Bringhurst, W. Jr., The Effect of Strand Size on Experimental Measurement of Solid Propellant Burning Rate Augmentation, M.S. Thesis, Naval Postgraduate School, Monterey, 1968.

8. NASA Report Number 66218, An Analytical Study of the Effects of Radial Acceleration Upon the Combustion Mechanism of Solid Propellant, by R. Glick, December 1966.

9. Summerfield, M., et al, "Burning Mechanism of Ammonium Perchlorate Propellants," Progress in Astronautics and Rocketry, v. 1, p. 142, 1960.

10. Project Squid Technical Report PR-114-P, A Phalanx Flame Model for the Combustion of Composite Solid Propellants, by J. Fenn, April 1967.

11. Schlichting, H., Boundary Layer Theory, p. 96-97, McGraw-Hill, 1955.

INITIAL DISTRIBUTION LIST

		No. Copies
1.	Defense Documentation Center Cameron Station Alexandria, Virginia 22314	20
2.	Library, Code 0212 Naval Postgraduate School Monterey, California 93940	2
3.	Commander, Naval Ordnance Systems Command Department of the Navy Washington, D. C. 20360	1
4.	Commander, Naval Air Systems Command Department of the Navy Washington, D. C. 20360	1
5.	Dr. David Netzer Department of Aeronautics Naval Postgraduate School Monterey, California 93940	2
6.	Lt. Robert Bates, USN 1415 West 103rd Street Los Angeles, California 90047	1

Security Classification

DOCUMENT CONTROL DATA - R & D

Security classification of title, body of abstract and indexing annotation must be entered when the overall report is classified)

1 ORIGINATING ACTIVITY (Corporate author)

Naval Postgraduate School
Monterey, California 93940

2a. REPORT SECURITY CLASSIFICATION
Unclassified

2b. GROUP

3 REPORT TITLE

The Effects of Acceleration on Burning Rates of Nonmetallized Composite Propellants

4 DESCRIPTIVE NOTES (Type of report and inclusive dates)
Master's Thesis; October 1969

5 AUTHOR(S) (First name, middle initial, last name)

Robert Carroll Bates

6 REPORT DATE	7a. TOTAL NO. OF PAGES	7b. NO. OF REFS
October 1969	70	11

8a. CONTRACT OR GRANT NO	9a. ORIGINATOR'S REPORT NUMBER(S)
b. PROJECT NO	
c.	9b. OTHER REPORT NO(S) (Any other numbers that may be assigned this report)
d.	

10 DISTRIBUTION STATEMENT

[redacted]

11 SUPPLEMENTARY NOTES	12. SPONSORING MILITARY ACTIVITY
*Approval granted only upon release by: Naval Ordnance Systems Command	Naval Postgraduate School Monterey, California 93940

13 ABSTRACT

The burning rates of five nonmetallized composite propellants were measured in acceleration fields up to 1000g using a combustion bomb mounted on a centrifuge. Two propellants were burned at 1000 psia and all five were burned at 500 psia.

The experimental results were examined to separate the effects of pressure, base burning rate and AP crystal size on burning rate augmentation. Increasing pressure was found to increase the augmentation except at low acceleration levels. The augmentation was found to be a strong function of base burning rate and a weak function of AP crystal size.

The results were compared with Sturm's model for augmentation of nonmetallized composite propellants and found to compare favorably. A new expression for $d_{critical}$ was proposed which better correlates experimental data.

DD FORM 1 NOV 65 1473 (PAGE 1)
S/N 0101-807-6811

Security Classification

A-31408

14 KEY WORDS	LINK A		LINK B		LINK C	
	ROLE	WT	ROLE	WT	ROLE	WT
Acceleration						
Burning Rate						
Non-metallized Composite Propellant						